https://doi.org/10.5194/egusphere-2025-1805
Preprint. Discussion started: 11 June 2025

Evaluation of North Atlantic Tropical Cyclones in a Convection-Permitting Regional Climate Simulation

Lara Tobias-Tarsh[1,2], Chunyong Jung[1], Jiali Wang[1], Vishal Bobde[3], Akintomide A. Akinsanola[1,3], V. Rao Kotamarthi[1]

[1]Environmental Science Division, Argonne National Laboratory, Lemont, IL, USA
[2]Department of Climate and Space Sciences and Engineering, University of Michigan, Ann Arbor, MI, USA
[3]Department of Earth and Environmental Sciences, University of Illinois Chicago, Chicago, IL, USA

Correspondence to: Lara Tobias-Tarsh (laratt@umich.edu) and Chunyong Jung (cjung2@anl.gov)

Abstract. This study employs a 20-year, convection-permitting (CP) regional climate model, forced by ERA5 reanalysis, to assess the representation and climatology of tropical cyclones (TCs) over the North Atlantic. We demonstrate that, relative to observations from Hurricane Database version 2 (HURDAT2), the model better captures TC frequency, averaging 12.25 TCs a year compared to 12.5 in HURDAT2 and 7.45 in ERA5. The model also successfully resolves the upper tail of the observed TC intensity distribution, while ERA5 only resolves TCs of Category 2 or lower intensity on the Saffir-Simpson scale. By contrast, the model and ERA5 show comparable skill at resolving the overall distribution of TC central pressure, implying that minimum central pressure may be a skillful predictor of TC intensity for coarser datasets. Spatially, the CP model exhibits particular added value over data-sparse coastlines in Central America and the Caribbean, successfully resolving clusters of TC track density that are missing in ERA5. Finally, a composite analysis of the 10 strongest TCs in each dataset, along with a case study of Hurricane Isabel (2003), reveals that TCs in the CP model have realistic structural features of the TC inner core that are not apparent in ERA5, including a more compact and intense radius of maximum wind. This is likely due to the CP model's enhanced capability to capture small-scale convection and storm structure. These improvements exemplify the represented CP model's efficacy for TC-induced local-scale hazard preparedness, and risk assessment of critical infrastructure, especially in regions lacking existing high resolution climate data.

1 Introduction

North America experiences a plethora of extreme weather throughout the year, with tropical cyclones (TCs) being particularly destructive due to their intense winds and heavy rainfall. Since their impacts are often localized, variations in land-use,

https://doi.org/10.5194/egusphere-2025-1805
Preprint. Discussion started: 11 June 2025

topography and coastal geometry can further exacerbate damage. TCs can also cause inland flooding, tornadoes (Schultz and Cecil, 2009; Franco-Diaz et al., 2019), and damage to offshore infrastructure (Worsnop et al., 2019; Hallowell et al., 2018).

Demand is therefore growing for detailed climate data able to accurately represent TC hazards at both synoptic and local scales. Such datasets are essential for risk assessment of critical infrastructure and for local government assessments of resilience to extreme weather. Limited computational resources, however, have restricted existing models — including global climate models (GCMs) with grid spacing of 30-100 km (IPCC, 2021) and regional climate models (RCMs) with grid spacing of ~10 km (e.g., Jacob et al., 2014)—from producing datasets at spatial and temporal resolutions fine enough to assess local or regional scale risks associated with extreme events. Due to their coarse grid spacing, these models rely on cumulus parameterization, a key source of uncertainty in numerical weather prediction models. This approach limits their ability to resolve meso- to micro-scale interactions critical for deep convection and creates complex nonlinear effects through interactions with other parameterization schemes, leading to biases that hinder realistic representation of convective phenomena like TCs.

Global reanalysis data provides a valuable resource for studying long-term TC trends and validating GCMs (Stansfield et al., 2020; Chand et al., 2022). These datasets combine observational data such as in-situ and satellite measurements with numerical model output to provide global coverage of conditions affecting TC track, including climatological oscillations and steering flows. They are also essential for supplementing inconsistencies in the observational record, which are particularly prevalent during TC genesis and extratropical transition (Hodges et al., 2017; Schreck et al., 2014). Although these datasets typically have higher spatial resolution than other GCMs, they are still too coarse to resolve deep convection and thus require cumulus parameterization (Jones et. al., 2021; Murakami, 2014). Previous studies (e.g., Stansfield et al., 2020; Tu et al., 2022) found that biases within reanalysis data are largest for the most intense TCs, resulting in a limited ability to capture realistic distributions of TC intensity. These limitations and biases may propagate into misrepresentation of TC-induced catastrophes, such as storm surge, flooding, and wind damages, which rely heavily on accurate TC intensity and structure.

A promising remedy for the deficient representation of TCs in reanalysis data involves utilizing convection-permitting (CP) RCMs with a horizontal grid spacing of 4 km or less. In order to achieve such fine resolution over a large spatial coverage and a long time span, these studies employ an approach known as dynamical downscaling, in which the relatively coarser reanalysis or GCMs are used to force boundary conditions over a limited area with a much higher spatial resolution. By explicitly resolving deep convection processes instead of relying on parameterization, these models show notable improvements (Prein et al., 2015), especially for deep convection-induced heavy rainfall, high wind speeds, and other phenomena with high spatiotemporal variability. Recent experiments at CP scales have also shown a better representation of TC dynamical and thermodynamic features, particularly in the inner-eye wall — the region where the lowest pressure and strongest winds (and thus the primary determinants of intensity) occur (Chen et al. 2007; Gentry and Lackmann, 2010; Hazelton et al., 2018; Kanada

https://doi.org/10.5194/egusphere-2025-1805
Preprint. Discussion started: 11 June 2025

and Wada, 2016; Kanada et al., 2020). Additionally, higher horizontal resolution enhances the modeling of TC and post-TC stages, such as extratropical transition (Jung and Lackmann, 2021, 2023; Liu et al., 2020).

With recent advancements in computational power and data storage, a number of decadal-scale CP RCM simulations have emerged, particularly focused on the contiguous United States (CONUS; Akinsanola et al., 2024; Gensini et al., 2023; Liu et al., 2017; Rasmussen et al. 2023). These simulations have demonstrated improvements in the representation of local-scale convective weather with sufficient temporal extent to conduct climatological studies. However, studies utilizing these simulations for decadal-scale climatologies have largely focused on land-based phenomena such as mesoscale convective systems (Rasmussen et al., 2023; Wallace et al., 2025) and supercells (Zeeb et al., 2024), with TCs often overlooked due to the large ocean domain needed to fully capture their lifecycle. Gutmann et al., (2018), to our knowledge, is the only study to examine North Atlantic hurricanes using a CP grid within a single continental-scale domain over a decade, demonstrating that these simulations could skillfully resolve TCs. However, their estimations of maximum wind speeds and minimum sea level pressure (SLP) exhibited a weak bias relative to observations, partly due to the coarse (~79 km) ERA-Interim boundary conditions advecting weak TCs into a limited ocean domain, reducing their opportunity for intensification before landfall. More recent, multidecadal CP-scale simulations (e.g. Akinsanola et al., 2024; Gensini et al., 2023; Rasmussen et al., 2023) have been forced by the European Centre for Medium-Range Weather Forecasting's Reanalysis Version 5 (ERA5; Hersbach et al., 2020). ERA5 has been shown to better represent TCs than the ERA-Interim dataset used to force HRCONUS, in part due to its higher horizontal resolution (Belmonte Rivas and Stoffelen, 2019; Malakar et al., 2020). As a result, TCs advected into their respective CP domains may be stronger and somewhat better defined. This may reduce the additional time needed for TCs to strengthen and allow TCs to reach more realistic intensities before landfall or dissipation. However, to the authors' best knowledge at the time of writing, the only CP-scale analyses of TCs forced by ERA5 employ event-based downscaling for individual TCs or use nested domains over the ocean (e.g. Steptoe et al., 2021), which may introduce additional boundary discontinuities that disrupt vertical motion at the interface between the convection-allowing inner domain and parameterized outer domain. Furthermore, despite these improvements, we note that ERA5 itself is still unable to produce TCs above Category 2 intensity (Stansfield et al., 2022). This may suggest that in the model, advected disturbances entering through the boundaries provided by ERA5 might necessitate a large ocean area to develop into strong TCs.

This study aims to evaluate North Atlantic TC climatology in one of these ERA5-forced multidecadal CP regional climate simulations: the Argonne Downscaled Data Archive V2 (ADDA_v2; Akinsanola et al., 2024), which outputs hourly over a uniform 4 km domain from 2001 to 2020. The ADDA_v2 domain spans the majority of North America and some of Central America, including Mexico and the surrounding Caribbean islands, as well as a large amount of the Northeast Pacific and Atlantic Ocean (Fig. 1). This domain is larger than other similar CP simulations (e.g. Gensini et al., 2023; Rasmussen et al., 2023), particularly over the open North Atlantic Ocean, providing ample space for TCs entering the domain to intensify in a CP configuration prior to interacting with the coast. Additionally, it covers regions that experience frequent TC landfalls and

https://doi.org/10.5194/egusphere-2025-1805
Preprint. Discussion started: 11 June 2025

are characterized by complex terrain with high heterogeneity in land-use and topography (Leroux et al., 2018). These regions often have high socioeconomic vulnerability to TC impacts yet have not previously been included in storm resolving simulations, perhaps due to insufficient observational data. These regions include many Caribbean islands and regions along the Gulf Coast of Central like Campeche and the Yucatan Peninsula (Dominguez et al., 2021; Hernandez Ayala et al., 2017; Hernandez Ayala and Matayas, 2018; Hidalgo et al., 2020). Access to CP-scale simulations in these regions are particularly important as the complex terrain and land-use can exacerbate TC impacts and increase uncertainty in risk assessment and emergency planning (Farfán et al., 2014; Rey et al., 2019; Smith et al., 2005).

Through comparison with observations from the revised Atlantic Hurricane Database (HURDAT2; Landsea et al., 2013), we investigate the ability of ADDA_v2 to simulate realistic TC climatology such as TC counts, intensity, and spatial distribution using metrics such as accumulated cyclone energy (ACE) over the past two decades. We also analyze composites of the ten strongest TCs simulated by ADDA_v2 and ERA5 to examine the added value of CP, high resolution simulations in representing TC structure. Additionally, through a case study of Hurricane Isabel (2003), we investigate the physical mechanisms behind the improvement in storm-scale TC representation observed in ADDA_v2, as compared to both observations and ERA5. While we do not expect ERA5 to capture all hurricane categories accurately, we aim to provide a comprehensive evaluation of its performance, identifying which categories pose challenges for ERA5 and determining the specific variables where it struggles, as well as those where it continues to represent hurricanes reasonably well.
The manuscript continues as follows: the methodology, including model description, validational datasets, and analysis metrics used in this study are outlined in Section 2, results of the model's performance at replicating TC characteristics are presented in Section 3, and a summary of our findings and avenues for future research are discussed in Section 4.

2 Methods

2.1 Model Description and Datasets

This study uses a continental-scale, CP regional climate model product (Akinsanola et al., 2024), developed using the Weather Research and Forecasting Model (WRF), version 4.2.1, to simulate 20 years of historical climate. The product domain covers 8200 × 7000 km, with a 4 km grid spacing encompassing North America and parts of Central America, including Alaska and Puerto Rico (Fig 1). Vertically, the simulation employs 50 unevenly spaced sigma levels, extending from the surface to 50 hPa, with 18 sigma levels concentrated below 1 km. Cumulus parameterization is excluded in favor of explicit convection. Initial, surface, and lateral boundary conditions are all derived from ERA5 data for the period 2001–2020, updated every 6 hours. Details of the WRF model configuration, including physical schemes and parameterizations, are documented in Akinsanola et al., (2024).
Evaluation of the ADDA_v2 and ERA5 data against observations is conducted primarily using the HURDAT2 database, which provides TC best position, minimum SLP, maximum sustained wind speeds and translation speed at 6-hourly intervals for the

https://doi.org/10.5194/egusphere-2025-1805
Preprint. Discussion started: 11 June 2025

entire study period (2001-2020). To examine storm structure for Hurricane Isabel (2003), we use the Tropical Cyclone Radar Archive of Doppler Analyses with Recentering (TC-RADAR) dataset (Fischer et al., 2022), an extensive database of airborne TC observations collected using the X-band tail Doppler radar aboard NOAA's WP-3D aircraft. This radar performs forward and backward scans, enabling detailed three-dimensional analyses of the inner-core structure of TCs. Each mission typically involves 3–4 passes through the storm center, generating storm-centered grids via a 'recentring' technique.

2.3 Tropical Cyclone Tracking

Tropical cyclones (TCs) in both ADDA_v2 and ERA5 are tracked using the automated TempestExtremes algorithm (Ullrich et al., 2021; Ullrich and Zarzycki, 2017; Zarzycki and Ullrich, 2017), following the procedure in Stansfield et al. (2020). First, local minima in SLP are identified as potential candidates, with weaker minima excluded if a deeper one exists within a 6° great-circle distance (GCD). Candidates must also exhibit a minimum SLP increase of at least 2 hPa within 5.5° GCD and a warm-core signature, defined as a ≥6 m decrease in 300–500 hPa geopotential thickness within 6.5° GCD of the local maximum in thickness.

Tracking is conducted over the full domain of each dataset and then restricted to the ADDA_v2 domain using a shapefile of the study domain. Consequently, some ERA5 and HURDAT2 TCs appear short-lived within ADDA_v2, and all datasets may include remnants crossing from the East Pacific. To focus on North Atlantic TCs, we only retain tracks with at least one point over ocean within the first 24 hours that falls inside the International Hydrographic Organisation (IHO) North Atlantic shapefile (Flanders Institute, 2018) and discard tracks starting over land. Tracks existing exclusively south of 12°N are removed to reduce boundary-related noise in ADDA_v2. To exclude extratropical cyclones, tracks entering the domain above 35°N or exceeding 50°N are discarded. Finally, tracks existing for fewer than two time steps (6 hours) are also discarded. We adopt a slightly higher latitude threshold (50°N) than Stansfield et al., (2020) as ADDA_v2 does not include the majority of the Atlantic Main Development Region (MDR; 10–20°N, 30–60°W), where many TCs initiate. As a result, we expect more recurving TCs to enter the domain later in their lifecycle, often at subtropical latitudes.

https://doi.org/10.5194/egusphere-2025-1805
Preprint. Discussion started: 11 June 2025

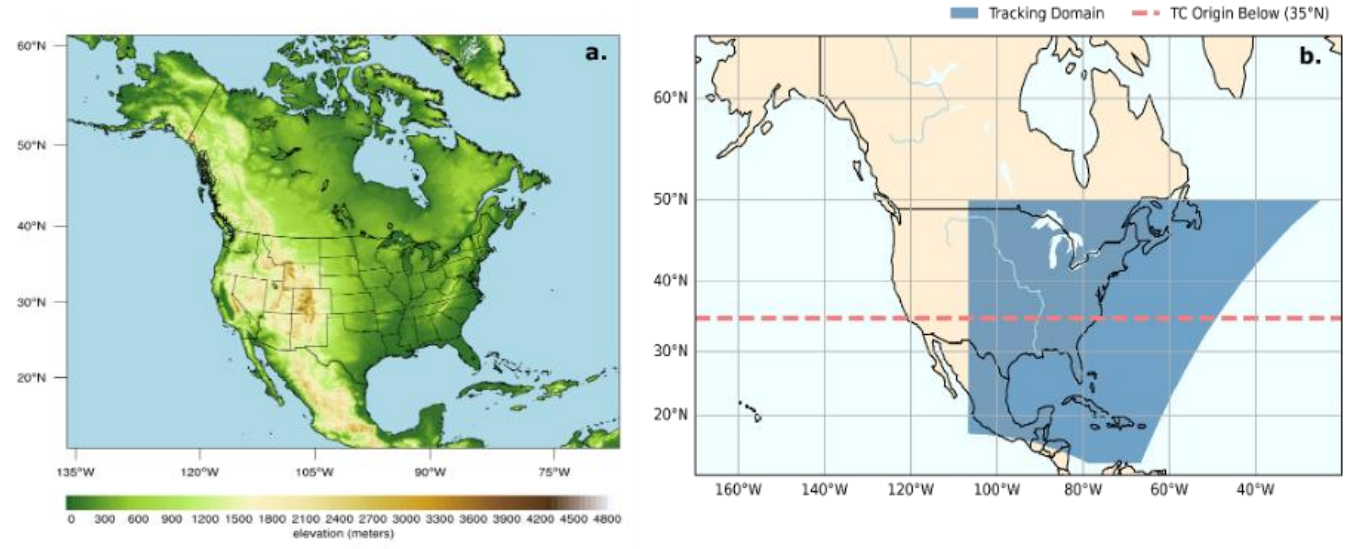

Figure 1: (a) WRF domain with terrain height for ADDA_v2. (b) Tracking domain for North Atlantic TCs in all datasets. The red line (35°N) delineates the location below which trajectories must enter into the domain to be considered TCs.

2.4 Tropical Cyclone Frequency and Metrics

TC counts are determined by summing the detected trajectories in each model for each year, while monthly average counts are used to demonstrate the ability to capture patterns of TC occurrence by calculating the arithmetic average of TC trajectories counts for each month of the 20-year period.

Frequency is also illustrated by calculating tropical cyclone days (TCDs), defined as any day in which one or more TC exist anywhere in the ADDA_v2 domain, and is broken down further based on TCs existing at each Saffir-Simpson scale category. This is particularly useful in comparing counts between the model data and HURDAT2 data, which may have some inconsistencies in the thresholds used to determine difficult to observe phases in the TC lifecycle when compared to the more controlled thresholds in the tracking data, for example genesis and extratropical transition.

Further summary of annual and monthly TC activity is quantified by determining the Accumulated Cyclone Energy (ACE), a valuable metric for assessing the intensity and duration of TCs, offering insights into their potential impact and associated risk (Bell et al., 2000; Villarini and Vecci, 2012). ACE is calculated as:

$$ACE = 10^{-4} \Sigma v^2{}_{max} \quad (1)$$

https://doi.org/10.5194/egusphere-2025-1805
Preprint. Discussion started: 11 June 2025

TC intensity is further analysed by employing the use of a simple wind-pressure relationship (WPR), which allows for a more comprehensive analysis of TC intensity by using traditional 10m wind-speed metrics and minimum SLP simultaneously. Additionally, this WPR may provide a greater insight into any biases observed in ERA5 or ADDA_V2 relative to the observed WPR, as we would expect coarser models like ERA5 to struggle more at representing the high wind speeds observed in the TC eyewall than minimum SLP (Chavas et al., 2017). Here, we fit the simple WPR outlined in Atkinson and Holliday (1979), which uses a power law relationship based on the cyclostrophic wind balance such that:

$$V_m = A(P_{env} - P_{min})^B \quad (2)$$

Where V_m is the TC maximum wind speed, P_{env} is the environmental pressure, set here to the 1020 mb estimate given in Atkinson and Holliday (1979) for the North Atlantic, P_{min} is the TC's minimum SLP, and A and B are fit coefficients to be determined.

2.5 Tropical Cyclone Spatial Variability

To further analyze spatial variability in the data, we determine the TC track density by binning TC centroids into 2.5 degree bins, and summing the total number of TC centroids existing in each bin over all 6-hourly timesteps. Other bin sizes were tested and produced similar results (Fig. S1). While the tracking domain does not cover the genesis location of many of the TC tracks, which we anticipate will enter from the MDR, we can use the initial and final points of detection to gain an understanding of a general trend in TC path and realistic track propagation.

2.6 Tropical Cyclone Structure

In addition to analyzing statistical TC climatology, we examine the differences in how ADDA_v2 and ERA5 represent storm-scale structures to assess the added value of CP simulations in capturing TC structure. We generate composites of the 10 strongest TCs in each dataset, following the method outlined in Bengtsson et al. (2007b) and Catto et al. (2010). These composite storms are derived from the simulated TCs at peak intensity (measured by minimum SLP) using a 300 km storm-centered coordinate. This storm-centered coordinate system is also used by TC-RADAR, allowing for direct comparison of individual storms in ADDA_V2 to observed TCs taking similar tracks. To further investigate the physical mechanisms underlying the differing representations of TCs between ADDA_v2 and ERA5, we focus on a single hurricane event—Isabel (2003). Hurricane Isabel (2003) stands out as one of the well-resolved hurricanes in ADDA_v2, enabling us to examine ADDA_v2's capability of simulating storm-scale structure in comparison with TC-RADAR and ERA5.

https://doi.org/10.5194/egusphere-2025-1805
Preprint. Discussion started: 11 June 2025

3 Results

3.1 Tropical Cyclone Frequency

We first compare TC counts at all intensities produced by ADDA_v2 and ERA5 to HURDAT2 (Fig. 2a). The 20-year mean TC counts in ADDA_v2 are closer to HURDAT2 (12.5 versus 12.25) than ERA5, which averages only 7.45. In particular, ERA5 always under-detects TCs, consistent with previous findings (e.g., Stansfield et al., 2020; Bie et al., 2021), while ADDA_v2 over-detects TCs in a number of years. ADDA_v2 reasonably captures the interannual variability in TC count, especially in years with abnormally high numbers of TC events, with a standard deviation of 4.13 compared to 4.94 observed in HURDAT2. ERA5 produces a standard deviation of 3.01 over the same period, and often undercounts TCs in years with many observed TC events (e.g., 2005, 2010 and 2011). In the mean seasonal cycle, both ADDA_v2 and ERA5 appear to successfully capture the seasonality of TC activity (e.g., peak season in September) in the domain (Fig. 2b), with similar median counts in each month. ADDA_v2 does generally capture the upper tail of the monthly distributions better when compared to its forcing data (ERA5), supporting the higher annual TC counts and suggesting an improved ability to capture the variability and extremes of TC activity.

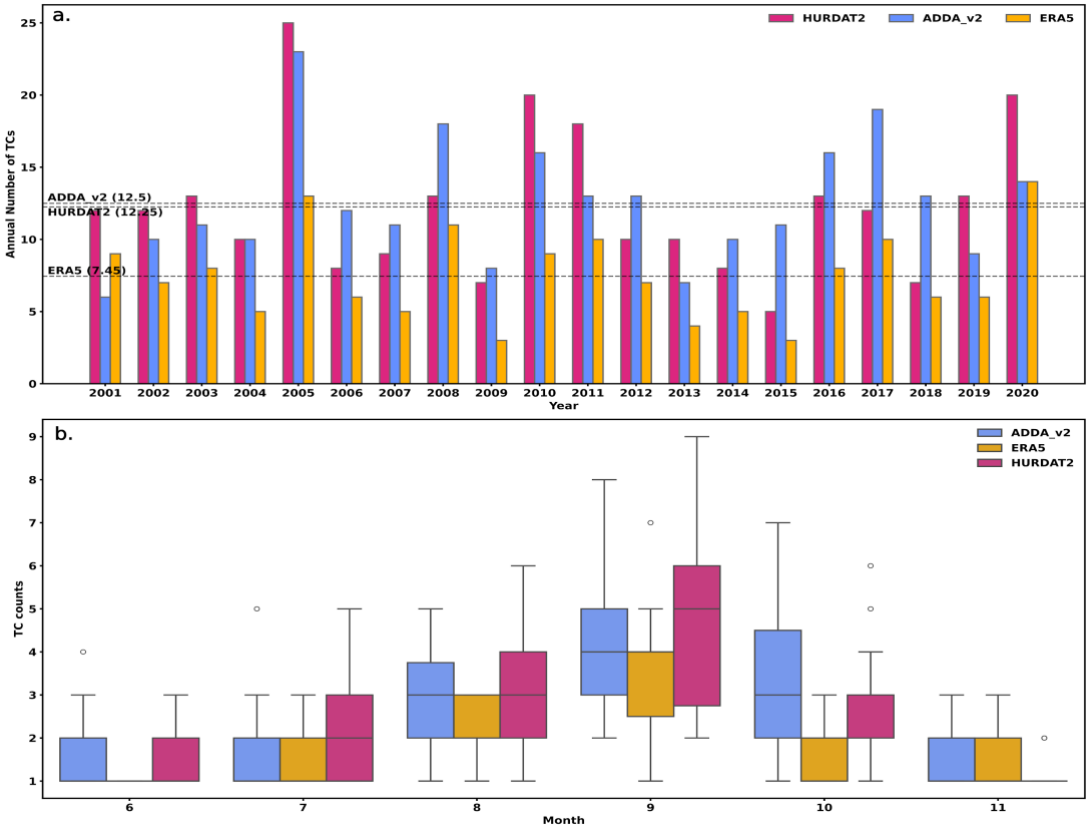

Figure 2. (a) Annual counts of TCs for HURDAT2, ERA5 and ADDA_v2 for the simulation period from 2001 to 2020. Dashed lines show the arithmetic average for the simulation period from 2001 to 2020. (b) box plot of TC counts in

https://doi.org/10.5194/egusphere-2025-1805
Preprint. Discussion started: 11 June 2025

each month during the hurricane season, boxes indicate 25th to 75th percentile, whiskers indicate 5th and 95th percentiles, circles indicate outliers, and lines within the box indicate the median monthly count.

ADDA_v2 continues to display an improved performance relative to ERA5 at representing the interannual variability of TC activity at different intensities. Figure 3a presents annual TC counts by maximum Saffir-Simpson category, with ADDA_v2 effectively reproducing the observed variability, including peaks in Category 1+ and 3+ hurricanes during 2005, 2011, 2017, and 2020. While ERA5 shows a similar but weaker pattern, it fails to simulate any TCs above Category 2 and overrepresents storms peaking at tropical storm intensity.

To account for TC lifetime, TC days (TCDs) are shown in Fig. 3b. Both ERA5 and ADDA_v2 capture the overall variability in annual TCDs, though ADDA_v2 more closely aligns with observations across all intensity categories. On average, ADDA_v2 overestimates TCDs above tropical storm intensity by 20 days, while ERA5 underestimates by 19.2 days relative to HURDAT2. At Category 1 intensity, ERA5 simulates only 3.45 TCDs annually (vs. 23.6 in HURDAT2) and fails to detect any TCDs above Category 2. ADDA_v2, by contrast, overestimates TCDs by 7 days at both tropical storm and Category 1 intensities, and by 5.79 days at Category 2. It performs well at major hurricane intensities, slightly underestimating Category 4–5 TCDs by just 0.21 days. This is likely due to the fact that ADDA_v2's domain is still small relative to the full Atlantic hurricane basin, meaning that some TCs advected into the domain may be resolved incorrectly or may not have enough time to intensify sufficiently before making landfall or exiting the domain.

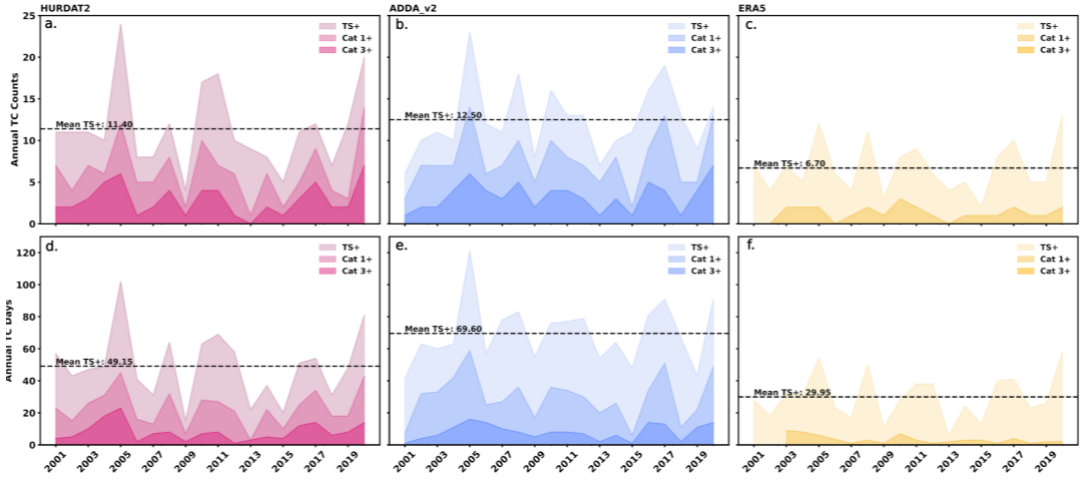

Figure 3: (a)-(c) annual TC counts and (d)-(f) annual TCDs for the simulation period for HURDAT2 (left), ADDA_v2 (middle), and ERA5. Groups based on the Saffir-Simpson scale into Tropical Storm (TS) or greater (> 18 m s^{-1}), Category 1 or greater (> 43 m s^{-1}) and Category 3 or greater (> 58 m s^{-1}).

https://doi.org/10.5194/egusphere-2025-1805
Preprint. Discussion started: 11 June 2025

While ADDA_v2's performance could be further improved through parameter tuning and resolution refinement, Fig. 3 shows that high-intensity TCDs remain underrepresented relative to observations. This may stem from the absence of the MDR in the ADDA_v2 domain, limiting storm intensification before and during advection across the boundary. In contrast, HURDAT2 tracks are not spatially constrained and may reflect stronger storms at the point of initial detection. Additionally, the combination of boundary and terrain effects may artificially extend the tracks of long-lived, landfalling TCs near the southern domain edge in Mexico's Sierra Madre mountains, despite filtering criteria requiring at least 10 track points below 150 m elevation. This "extension" leads to an erratic inland TC track over the high terrain following a realistic over-ocean track and landfall location, which we hypothesise may inflate TCDs at TS intensity and below (Fig. S2). Tracking TCs over complex terrain is inherently challenging, as is verifying inland tracks due to sparse observational data and inconsistencies in the best track data (Schreck et al., 2014), thus we retain these inland tracks while acknowledging their contribution to a potential high TCD bias. Moreover, a subset of ADDA_v2 (and ERA5) tracks may capture the extratropical transition phase, where residual warm-core structure leads to continued detection by TempestExtremes despite non-tropical characteristics (Jung and Lackmann, 2021). These cases can exhibit TS-strength winds, further contributing to TCD overestimation. Despite these limitations, ADDA_v2 exhibits a more realistic representation of TC activity and intensity in response to large-scale environmental conditions compared to ERA5. Since ADDA_v2 is driven by ERA5 boundary conditions, its improved depiction of TC intensities highlights the added value of the CP-scale downscaling approach.

3.2 Spatial Distribution of Tropical Cyclones

To understand the spatial climatology of TCs in each dataset, we analyze the track density, location of initial TC positions and average translation speed and vectors over the domain over the 20 years. Figs. 4(a)-(c) show track density in each dataset. ADDA_v2 better captures the magnitude of track density relative to HURDAT2 than ERA5, resolving clusters of TC activity in landfall regions such as the Bay of Campeche, the coast of Honduras and the Caribbean Islands and near the southeast Gulf Coast. We also find a cluster over the western Atlantic south of Bermuda in the region where Atlantic TCs often recurve. It is found that ADDA_v2 shows a more accurate spatial distribution of TCs than ERA5 relative to HURDAT2, with track density showing RMSEs of 9.92 and 11.31 counts per grid cell respectively. ADDA_v2 also consistently improves precision difference, mean error, modeling yield and scores a near perfect Q95 difference (Table S1), again indicating a better representation of spread and extremes in TC activity, which is much lower in ERA5 across most grid cells. While we select 2.5 degree bins to highlight broader climatological patterns across the domain, we observe similar results regardless of the bin size used across the domain (Fig. S1, Table S1).

To examine the realism of the TC tracks depicted in ADDA_v2, we assess the initial position of TCs detected in the domain (Figs. 4d-f) and the translation vectors (Figs. 4g-i) of each TC track over the full period. All three datasets capture a cluster of TCs with initial locations near the eastern edge of the tracking domain, where depressions and TCs are likely to be entering from the Atlantic MDR. While we expect HURDAT2 and ERA5 to be able to capture this without issue, we note that

https://doi.org/10.5194/egusphere-2025-1805
Preprint. Discussion started: 11 June 2025

ADDA_v2 also captures this signal, increasing confidence that TCs crossing into the model domain from the MDR are detected. However, the higher densities in ADDA_v2 on the eastern domain boundary may indicate possible boundary noise. All datasets also show a secondary cluster in the Gulf of Mexico, which is more pronounced in ADDA_v2 and least visible in ERA5. TC propagation direction following their detection is generally consistent across all three datasets (Figs. 4g-i), and is consistent with climatologically characteristic TC track patterns. TCs over the portion of the west North Atlantic contained in the model domain demonstrate a "recurving pattern" as they propagate northward, indicating the representation of realistic large-scale steering flows in the model domain. A small region of the southern Gulf of Mexico exhibits a straighter, east to north-eastward propagation pattern consistent with tracks generally making landfall in Central America and Northern Mexico.

Translation vectors become more variable and the average translation speed increases with northward extent – particularly above 40°N – in all datasets, similar to the findings of Zhang et al., (2020) in all basins. It is worth noting that while ERA5 does not contain any TC specific data assimilation (Hodges et. al., 2017), ERA5 necessarily assimilates observations—including corrected data - at every timestep (Hersbach et. al., 2020). Slocum et. al., (2022) demonstrate that, especially in the North Atlantic where routine reconnaissance missions are conducted to increase the density of observations around TCs and tropical disturbances for operational purposes, TC tracks in ERA5 are spatially very close to their HURDAT2 position. By contrast, ADDA_v2 has its own internal and spatial variability, thus tracks cannot be accurately "matched" to observations. ERA5 outperforms ADDA_v2 for pattern correlation across all spatial metrics (Table S1, S2), for example, scoring 0.90 for track density relative to ADDA_v2's 0.84. This is likely because the tracks of TCs detected in ERA5 are inherently close to HURDAT2 due to the aforementioned data assimilation process. This is supported by the noticeable decrease in ADDA_v2's pattern correlation relative to ERA5 with smaller bin sizes, as increasing the number of bins places higher weight on individual tracks (Fig. S1, S2). Moreover, ERA5 outperforms ADDA_v2 in representing TC translation speed and initial position, showing lower RMSE and higher pattern correlation (Table S2). This is likely due to ERA5's global domain, which more faithfully captures upper-level steering flows, while ADDA_v2 develops its own internal variability within its limited tracking domain.

https://doi.org/10.5194/egusphere-2025-1805
Preprint. Discussion started: 11 June 2025

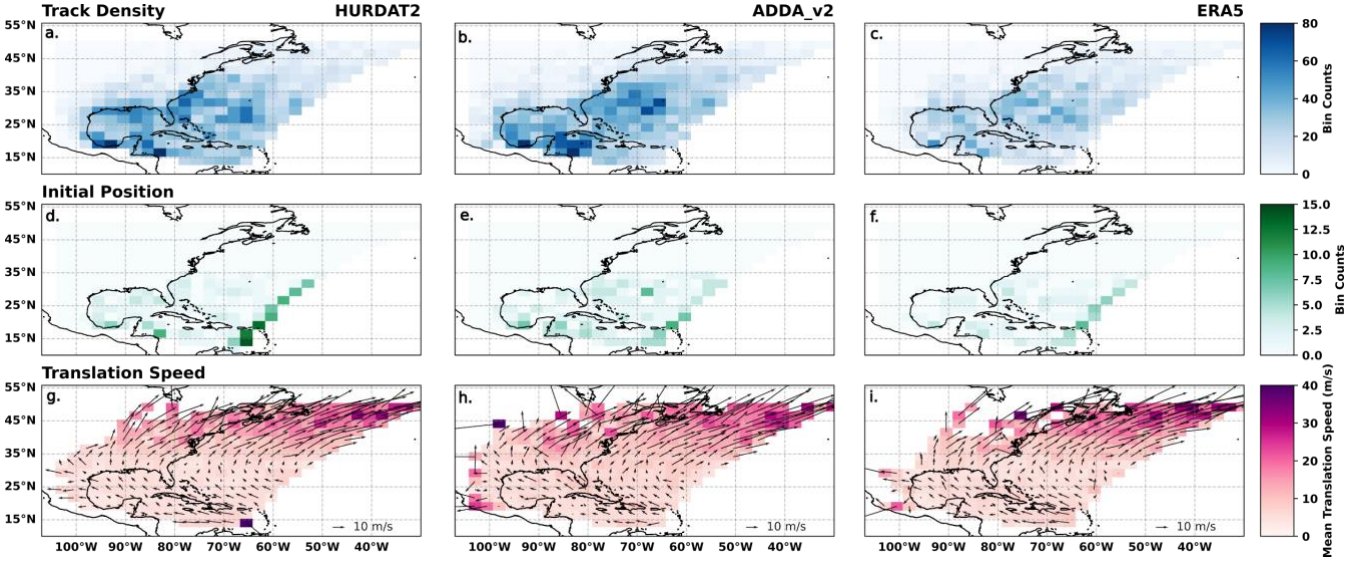

Figure 4: (a)-(c) Track Density, (d)-(f) Initial TC locations, and (g)-(i) Average TC translation speed (shading; m s-1) and vector (arrow) for the full study period in (a), (d) and (g) HURDAT2, b, e and h) ADDA_v2 and (c), (f) and (i) ERA5.

3.3 Tropical Cyclone Intensity: Maximum 10-m Wind Speed and Minimum SLP

Fig. 5 shows the distributions of 10 m wind speeds and minimum SLP at the TC center, which are the two parameters traditionally used to denote TC intensity, along with the WPR for each dataset. For reference, an intensity scale is added to each distribution, with the traditional Saffir-Simpson scale used for maximum 10 m wind speed, and the revised TC intensity scale proposed by Klotzbach et al., (2020) used for the minimum SLP distribution. In order to maintain a reference environmental pressure of 1020 mb in accordance with Atkinson and Holliday (1979), this figure excludes all points with minimum SLP values below 1020 mb (a total of 6 points in HURDAT2, 7 points in ADDA_V2, 0 points in ERA5).

The minimum SLP distributions have a relatively similar shape across all three datasets, though ADDA_v2 performs slightly better than ERA5, with a skewness error of -0.38 versus -0.57, and an overlapping ratio of 0.93 versus 0.87, respectively, relative to HURDAT2 (Fig. 5a). The maximum wind speed distributions reveal a more pronounced difference between ADDA_v2 and ERA5. Specifically, ERA5 again exhibits a greater skew error of 0.86, compared to 0.34 in ADDA_v2. Indeed, we observe that the shape of the ERA5 distribution is compressed, resulting in an overlapping ratio of 0.72 with HURDAT2. ADDA_v2 more closely captures the shape and tails of the observed HURDAT2 distribution, especially for strong TCs, resulting in a higher overlap ratio of 0.83. Nonetheless, both datasets exhibit a bias towards Saffir-Simpson Scale intensities of below Category 1, indicating that ADDA_v2 does inherit some of the weak bias from ERA5.

https://doi.org/10.5194/egusphere-2025-1805
Preprint. Discussion started: 11 June 2025

The fitted WPR curves support this further, showing ADDA_v2 and ERA5 to exhibit similar patterns of exponential decay owing to the small difference in B coefficient, while HURDAT2's WPR decays more slowly. In ADDA_v2, TCs below Category 1 on both scales tend to exhibit higher minimum SLPs and stronger winds than either of HURDAT2 or ERA5, which is likely a function of TCs advected into the domain strengthening with the removal of the CP constraints contained in the forcing data. Furthermore, ADDA_v2 still struggles to capture the strongest TCs, with fewer reaching Categories 4 and 5 on either scale than HURDAT2 (Table S4, S5). Moreover, we note that while the ADDA_v2 and ERA5 distributions for both intensity metrics are significantly different at $P < 0.001$ and that ADDA_v2 does still struggle to capture Category 5 TCs on both scales, ADDA_v2 scores a lower test statistic on all three nonparametric goodness of fit tests for the minimum SLP, 10 m wind, and WPR-calculated distributions (Table S3), indicating that ADDA_v2's distribution is a comparatively better fit than ERA5 for the observed distribution of TC intensity over the study domain. The improved representation of the distribution of intense TCs demonstrates the added value of allowing explicit convection on TC intensity in ADDA_v2 at resolving the climatology of intense TCs.

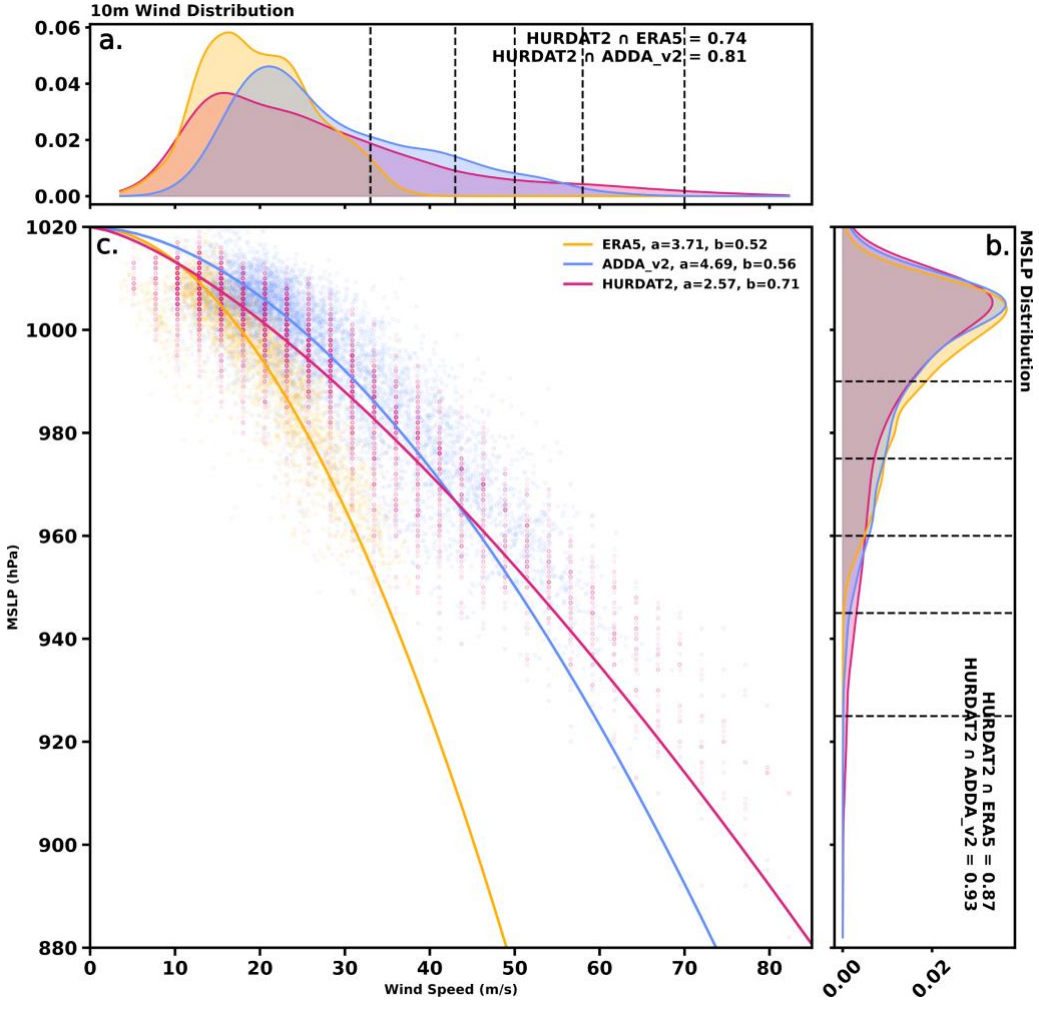

https://doi.org/10.5194/egusphere-2025-1805
Preprint. Discussion started: 11 June 2025

Figure 5: Kernel density estimate smoothed Probability Density Functions (PDFs) of minimum SLP (b) and 10m wind speeds (a), with a relative to the fitted WPR (c). The reference intensity scales are the Klotzbach et al. (2020) revised minimum SLP based scale for the minimum SLP distribution, and the standard Saffir-Simpson wind speed scale for the 10m wind distribution. The overlapping area is calculated as the integral between the model PDFs and the observed HURDAT2 PDF.

3.4 Tropical Cyclone Intensity: Accumulated Cyclone Energy (ACE)

To further examine the ability of ADDA_v2 to represent the distribution of TC intensity, we analyze the distribution of ACE. ADDA_v2 and HURDAT2 resolve higher annual ACE in the domain than ERA5 (Fig. 6). The mean error in annual ACE over the 20 years relative to HURDAT2 is -6.28 kt2 in ADDA_v2, and -72.5 kt2 in ERA5. In particular, we note that even in years where ERA5 performs relatively well at representing TC count such as 2001 and 2020, ACE is still drastically underestimated. Both ADDA_v2 and ERA5 also capture the pattern of interannual variability in ACE. ERA5, however, is unable to capture the magnitude of this variability, with a standard deviation of 14.5 kt2 compared to 54.3 kt2 in HURDAT2 and 46.6 kts2 in ADDA_v2. The spatial distribution of ACE over the full tracking period shows a similar pattern to the annual accumulated ACE statistics. Much like with track density and translation speed, spatial pattern correlations are higher in ERA5 (0.73) than ADDA_v2 (0.61) as the tracks are not independent of observations in ERA5, however ERA5 underestimates ACE more than ADDA_v2 (RMSE: 0.24 versus 0.2) in the majority of grid cells. ERA5 is unable to capture any maxima in ACE with a low standard deviation across bins of 0.07 in average ACE compared to 0.2 in HURDAT2, and 0.15 in ADDA_v2.

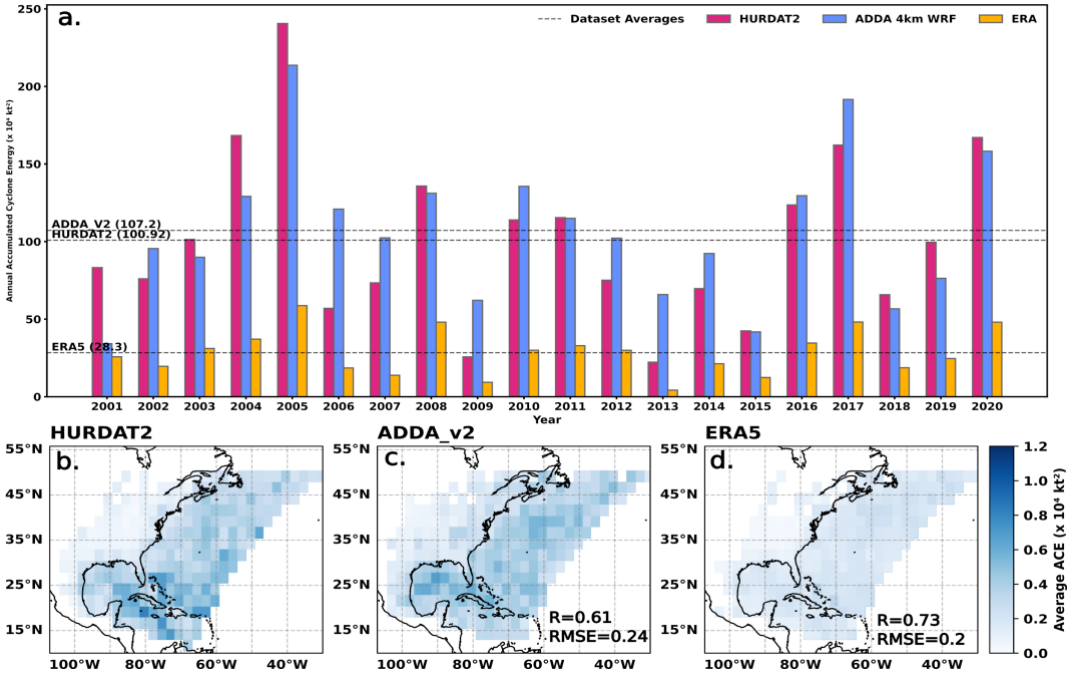

https://doi.org/10.5194/egusphere-2025-1805
Preprint. Discussion started: 11 June 2025

Figure 6: Accumulated Cyclone Energy (b, c, and d) annually averaged per grid cell for the full domain and summed for the full 20 year period (a). ACE is calculated using 2.5 degree bins.

3.6 Mechanisms Behind the Improvement in ADDA_v2

As previously shown, a key advantage of convection-permitting (CP) simulations lies in their improved ability to capture TC climatology, particularly at higher intensities. This stems from better resolution of storm-scale structure and the explicit representation of deep convection, which is otherwise suppressed by cumulus parameterizations and hydrostatic assumptions in coarser models (Gentry and Lackmann, 2010; Reed and Jablonowski, 2011, 2012; Zarzycki and Jablonowski, 2014; Zhang and Wang, 2018). To assess the added value of CP resolution, we compare composite TC structure in ADDA_v2 and ERA5. We further explore the mechanisms behind structural representation by evaluating both against TC-RADAR observations for one of the TCs that is simulated relatively faithfully in ADDA_v2—Hurricane Isabel (2003).

3.6.1 Composite Storms

Fig. 7 shows vertical profiles of azimuthally averaged composites depicting temperature anomaly (relative to the mean over a 300 km storm-centered domain), vertical velocity, and tangential and radial winds for both datasets. While both composites exhibit typical TC features—such as upward motion along the eyewall, radial surface inflow with outflow at the storm top, and strong cyclonic flow peaking in the lower troposphere—clear differences emerge between ADDA_V2 and ERA5. ADDA_V2 shows a distinct warm core throughout the troposphere, with a maximum temperature anomaly of 12.5 K around 450 hPa (Figs. 7a–b). By contrast, ERA5 displays two warm cores at different vertical levels in the mid-troposphere, inconsistent with satellite and dropsonde observations (e.g., Wang and Jiang, 2019). A plausible reason for ERA5's underperformance in simulating strong TCs (e.g., > Category 2) may be that its cumulus parameterization misplaces the height of maximum heating, inhibiting intensification. ADDA_V2's convection-permitting resolution better resolves inner-core pressure gradients, enhancing boundary layer moisture flux, convergence, and latent heat release throughout the troposphere (Manganello et al., 2012). This results in more intense warming and a higher temperature anomaly peak in ADDA_V2, aligning with Wang and Jiang (2019).

According to the well-defined warm core structure, ADDA_v2 displays comparable increases in the radial velocity of composite storms, reaching a maximum of 47.1 m s^{-1}, along with associated ascending motion exceeding 1.0 m s^{-1} in the upper troposphere (Fig. 7c). In contrast, ERA5 shows a lower peak radial velocity of 16.0 m s^{-1} and vertical motion of 0.46 m s^{-1} in the mid-troposphere (Fig. 7d), potentially linked to the lower maximum temperature anomaly height discussed earlier. The slope of the azimuthally averaged eyewall updraft is shallower in ADDA_v2 compared to ERA5 (Figs. 7c–d), consistent with a smaller radius of maximum wind (RMW) and greater vertical extent of strong tangential winds (Figs. 7a–b; Stern and Nolan, 2009). Both datasets exhibit cyclonic tangential winds throughout the troposphere, peaking near 850 hPa; however, differences are evident in magnitude and RMW—48.2 m s^{-1} and 114 km in ERA5 versus 59.7 m s^{-1} and 62 km in ADDA_v2.

https://doi.org/10.5194/egusphere-2025-1805
Preprint. Discussion started: 11 June 2025

The composite storm in ADDA_v2 corresponds to a Category 4 TC (59.7 m s^{-1}), while ERA5 aligns with Category 2 (48.2 m s^{-1}). Based on Hsu and Yan (1998), mean RMWs are typically 46 km for Category 2 and 48 km for Category 4 hurricanes. ADDA_v2 reasonably represents RMW for its strongest composite storms, whereas ERA5 depicts TCs with RMWs more than twice the typical size for storms of similar intensity—consistent with known biases in coarse-resolution datasets (Schenkel and Hart, 2012; Chavas et al., 2017). Figs. 7e–f further support this, as ERA5 exhibits a broader, less organized precipitation field with a peak of 22 mm hr^{-1}, while ADDA_v2 reaches 40 mm hr^{-1} in the southwestern quadrant of the eyewall. ADDA_v2 also presents more realistic convective features, including organized banding and a distinct rain-free eye—features absent in ERA5. These results reinforce ADDA_v2's enhanced ability to capture TC structure.

https://doi.org/10.5194/egusphere-2025-1805
Preprint. Discussion started: 11 June 2025

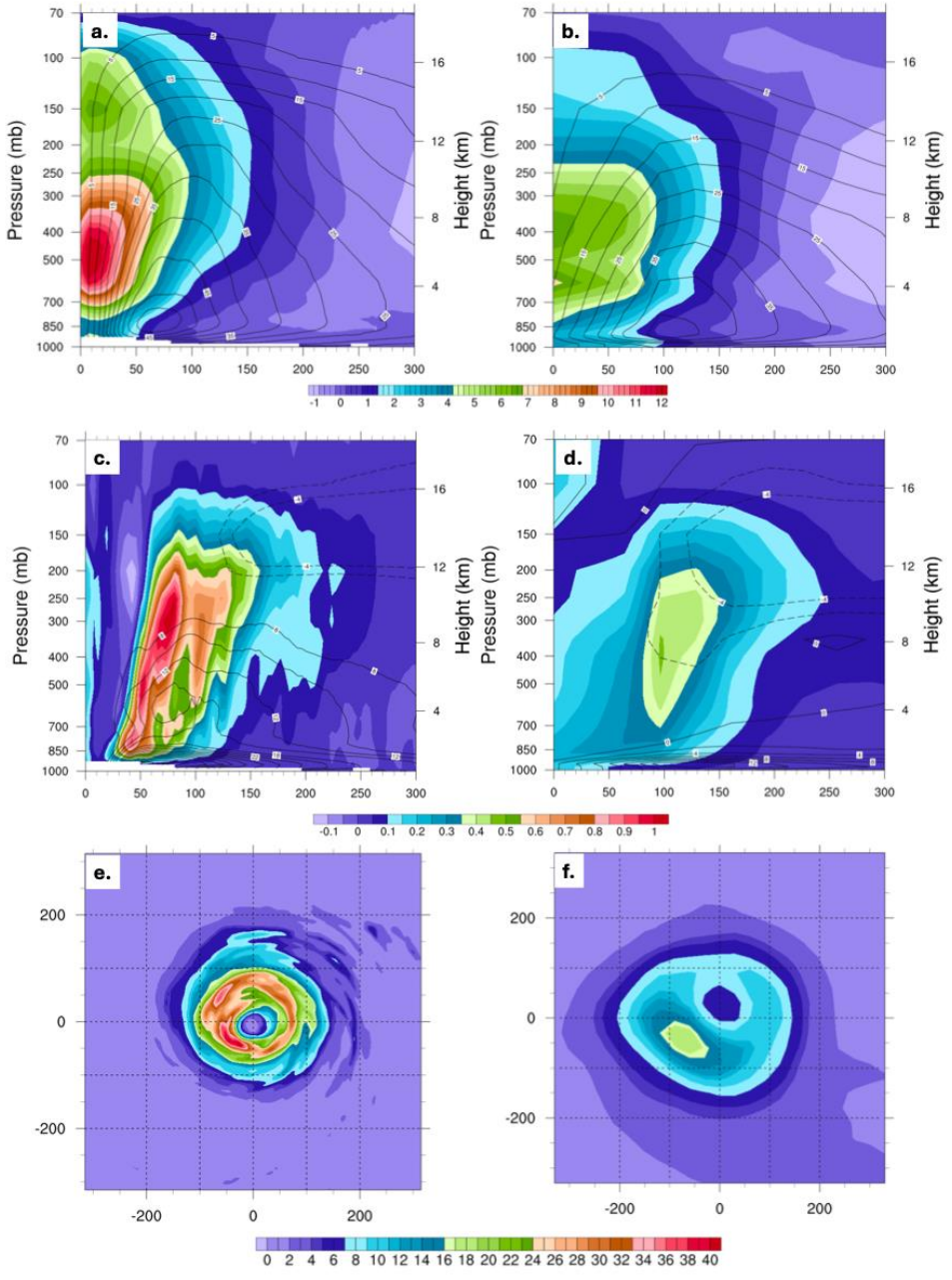

Figure 7: (a)-(b) Radial-height cross section of the azimuthally averaged temperature anomaly (shadings; K) and tangential wind speed (contours; m s^{-1}). (c)-(d) Radial-height cross section of the azimuthally averaged, and vertical velocity (shadings; m s^{-1}) and radial wind speed (contours; m s^{-1}). (e)-(f) Spatial pattern of hourly precipitation near the storm areas. The profiles are derived from the composite of the 10 strongest storms in ADDA_v2 (left column) and ERA5 (right column), respectively.

https://doi.org/10.5194/egusphere-2025-1805
Preprint. Discussion started: 11 June 2025

3.6.2 Hurricane Isabel - Assessing Storm Structure: ADDA_v2, ERA5, and TC-RADAR Comparisons

Fig. 8 shows the track of Hurricane Isabel in all three datasets. ADDA_v2 and ERA5 underestimate the observed storm's intensity. However, ADDA_v2, while deviating from the observed track, mitigates the intensity underestimation seen in ERA5. The simulated storm in ADDA_v2 reaches Category 4 (~62.3 m s^{-1}), while ERA5 captures Category 3 intensity (~50.3 m s^{-1}) on the Saffir-Simpson scale at their peak times. After 00 UTC on 16th September, ADDA_v2 shows weaker intensity as the storm accelerates post-peak and makes landfall earlier, placing it in different environmental conditions (e.g., SST, storm-land interaction) compared to ERA5. Therefore, we focus on the time when the observed storm reached peak intensity (19 UTC on 14th September), as both storms in ADDA_v2 and ERA5 are either at or near their peak intensities and are in close proximity to the observed track at this time.

In comparison with TC-RADAR and ERA5, ADDA_v2 shows clear improvement in storm structure representation both horizontally and vertically (Fig. 9). It accurately captures the shape, size, and intensity of observed relative vorticity, unlike ERA5, where these features are less distinct (Figs. 9a-c). The strong vorticity annular ring in ADDA_v2 matches the observations well, both in horizontal distribution and vertical profile (Figs. 9a-c, j-l). In TC-RADAR, irregular vorticity segments appear as small-scale vortices or mesovorticies within the eyewall (Fig. 11a), potentially associated with vortex Rossby waves (VRWs). While these features are not clearly seen in ADDA_v2, the presence of the polygonal cyclonic relative vorticity along the eyewall in ADDA_v2 suggests the possibility of breaking VRWs (Fig. 9b; Kossin and Schubert, 2001; Wang, 2002). This could be due to ADDA_v2's ability to resolve a broader range of wavenumbers (e.g., Gentry and Lackmann, 2010). Additionally, ADDA_v2 captures vertical motions better than ERA5, including both symmetric and asymmetric components (Figs. 9d-f). ERA5 fails to adequately capture vertical motions, especially with an expanded radius of maximum motion (~60km), while ADDA_v2 shows numerous smaller upward velocity maxima and adjacent downward motions adjacent to the ring of ascent the eyewall (Figs. 9e,n). TC-RADAR also shows these features, which ADDA_v2 replicates more accurately. It is worth noting that vertical velocity analyses for storms prior to 2010 in TC-RADAR are known to contain potential errors, which, in some instances, result in overly deep and strong storms (Fischer et al., 2023). Nevertheless, it is clear that ADDA_v2 demonstrates a well-defined symmetric updraft ring in the eyewall, along with numerous embedded updrafts and downdrafts across the eyewall, as observed in previous studies (e.g., Fierro et al., 2009; Gentry and Lackmann, 2010; Fig. 9e).

ADDA_v2's wind speed distribution, both horizontally and vertically, closely matches TC-RADAR, with a maximum wind speed of 83.6 m s^{-1} and a radius of 43.4 km (similar to TC-RADAR's 74.6 m s^{-1} magnitude and 43.1 km radius) at 1-km above the ground. (Figs 9g-h). In contrast, ERA5 overestimates the radius by 28.5 km (ERA5 radius: 71.6 km) and underestimates the magnitude by 15.2 m s^{-1} (ERA5 wind speed: 59.4 m s^{-1}) relative to TC-RADAR at the altitude at this time (Fig. 9i). Additionally, ADDA_v2 better resolves the vertical wind structure in the eyewall, peaking around 1 km, similar to TC-RADAR

https://doi.org/10.5194/egusphere-2025-1805
Preprint. Discussion started: 11 June 2025

(Figs. 9p-r). As observed in the TC composites, this might be likely due to ADDA_v2's higher resolution, as ERA5 tends to represent larger, weaker TCs.

3.6.3 Hurricane Isabel - Physical Processes behind the Improvement in ADDA_v2

To explore the processes behind ADDA_v2's improved representation of Hurricane Isabel, we computed radial averages of boundary layer (BL) integrated inflow and vertical mass flux for both ADDA_v2 and ERA5 at 19 UTC on 14th September (Table 1). Compared to ERA5, ADDA_v2 generates a significantly larger low-level inward mass flux, which, in accordance with mass conservation, corresponds to a larger vertical mass flux in the eyewall (Table 1). This suggests that the secondary circulation in ADDA_v2 is stronger (Fig. 9q), which corresponds with the larger simulated sensible and latent heat fluxes, conditions that are favourable for storm intensification (Fig. 10). As air moves towards the storm center, the conservation of angular momentum increases its speed, resulting in stronger winds and a more robust storm structure in ADDA_v2 compared to ERA5 (Fig. 9). This leads to higher integrated BL kinetic energy, defined by Powell and Reinhold (2007), in ADDA_v2 (Table 1), indicating greater damage potential. Therefore, ADDA_v2's representation of Hurricane Isabel suggests more significant impacts, such as wind damage and storm surge, highlighting the importance of CP regional climate modeling for accurate hurricane risk assessment.

The proposed interactive processes are tied to heat transfer from the ocean to the atmosphere, with SST playing a key role. We examine SSTs in a 300 km × 300 km storm-centered coordinate (Figs. 12c,f). At 19 UTC on 14th September, ADDA_v2's storm is over slightly colder SSTs (28.2°C for the spatially averaged SST) compared to ERA5 (28.6°C for the spatially averaged SST). This suggests that, despite the colder SSTs in ADDA_v2, more efficient surface heat transfer occurs, leading to a greater inflow mass flux as well as secondary circulation (Fig. 10). These factors contribute to stronger storm intensification and robust storm structure compared to ERA5. Another factor that significantly influences storm development is vertical wind shear. It is well documented that strong vertical wind shear can inhibit the intensification of TCs by tilting the storm's vertical structure. This tilting disrupts the alignment of the storm's core, reducing the efficiency of the heat engine and limiting intensification (e.g., Bi et al., 2023). Therefore, if the two storms experience different shear conditions, such as ERA5 being in a stronger shear environment, it could lead to weaker intensity and a less organized structure in ERA5. To investigate further, we calculate the shear between 850 and 200 hPa using wind components averaged over a 300 km radius from the storm center, following Braun and Wu (2007). Fig. 11 shows the time series of 850-200 hPa shear and minimum SLP for both datasets from 00 UTC on 14th to 00 UTC on 15th September 2003. The shear difference remains insignificant throughout, though ADDA exhibits higher shear than ERA5 until 18 UTC on 14th, when both ADDA_v2 and observed storms reach peak MLSP, 3 hours earlier than the storms in ERA5. Thus, wind shear does not appear to influence the weak intensification in ERA5.

Possible explanations for the different intensification pathways between the two storms, despite similar environmental conditions (e.g., SST, vertical wind shear), may lie in ADDA_v2's improved representation of small-scale convection (Figs. 9e-f). CP scale models can resolve these smaller convective processes, which coarser models must parameterize. These small-

https://doi.org/10.5194/egusphere-2025-1805
Preprint. Discussion started: 11 June 2025

scale updrafts and downdrafts enhance vertical mixing, allowing for more efficient heat and moisture transfer from the surface to the atmosphere. CP scale models capture finer details of the near-surface wind field, including localized changes in wind speed and direction, which enhance heat exchange at the atmosphere-ocean interface and in the boundary layer. This improved feedback results in more realistic enthalpy heat flux exchanges, crucial for TC development, leading to a better representation of TCs in the model.

Table 1: The first two columns display the radially averaged BL integrated inflow and vertical mass fluxes (kg m^{-1} s^{-1}) within a height of 1.2 km and a radius of 60 km from the storm center. The third column presents the radially BL integrated kinetic energy within a height of 1.2 km and a radius of 120 km from the storm center.

Data	BL Inflow mass flux (kg m^{-1} s^{-1})	BL vertical mass flux (kg m^{-1} s^{-1})	BL kinetic energy (kg m^{2} s^{-2})
ADDA_v2	-4.28×10^5	4.64×10^5	3.87×10^7
ERA5	-1.12×10^5	1.21×10^5	1.10×10^7

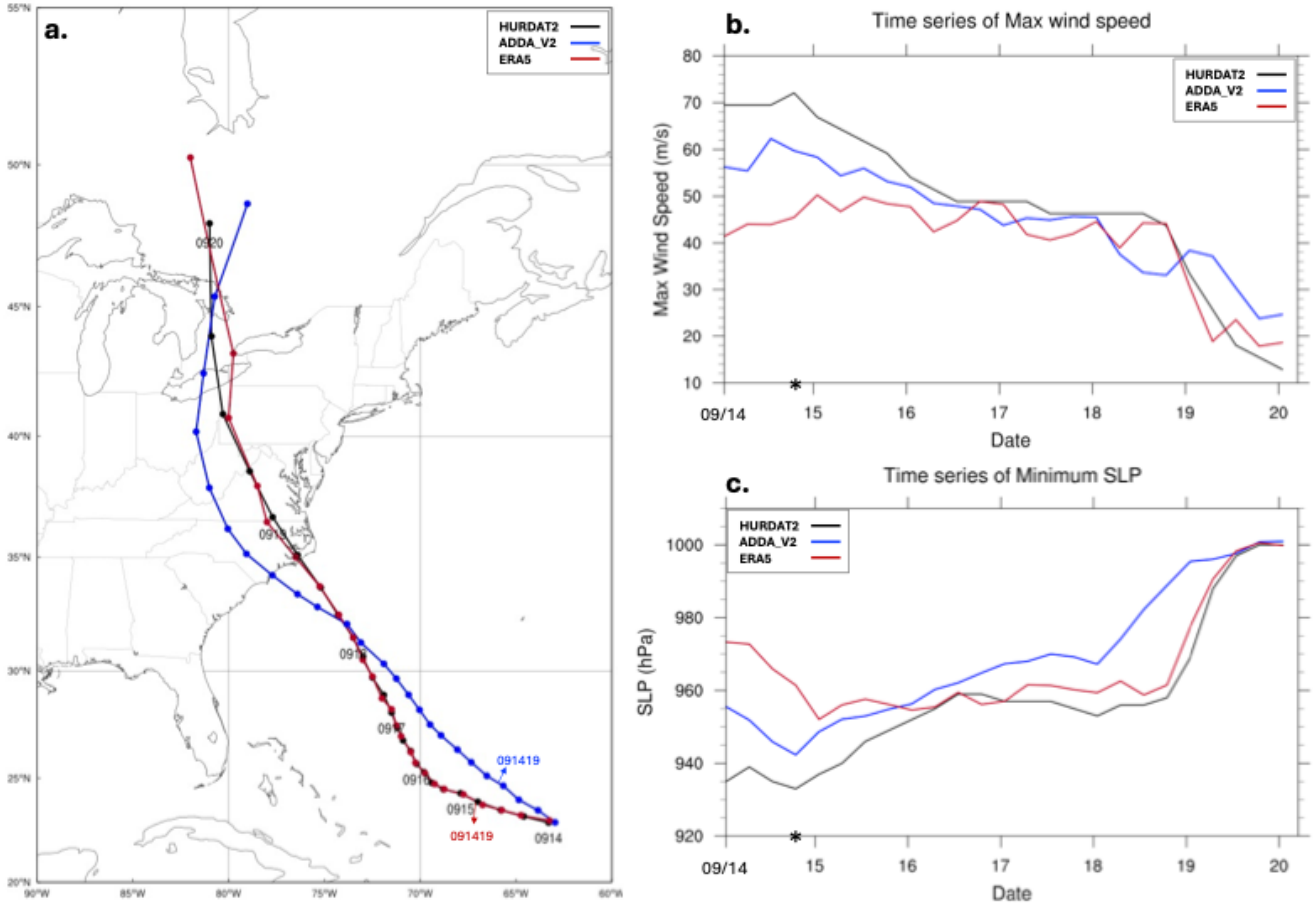

Figure 8: Comparison of (a) track, (b) time series of maximum wind speed (m s^{-1}) at 10-m, and (c) time series of minimum SLP (hPa) for Hurricane Isabel (2003) against observations. Black lines indicate values derived from HURDAT2, while blue and red lines

https://doi.org/10.5194/egusphere-2025-1805
Preprint. Discussion started: 11 June 2025

represent values derived from ADDA_v2 and ERA5, respectively. The time at which storm structure comparisons between the gridded data with TC-RADAR were made are indicated by asterisks.

https://doi.org/10.5194/egusphere-2025-1805
Preprint. Discussion started: 11 June 2025

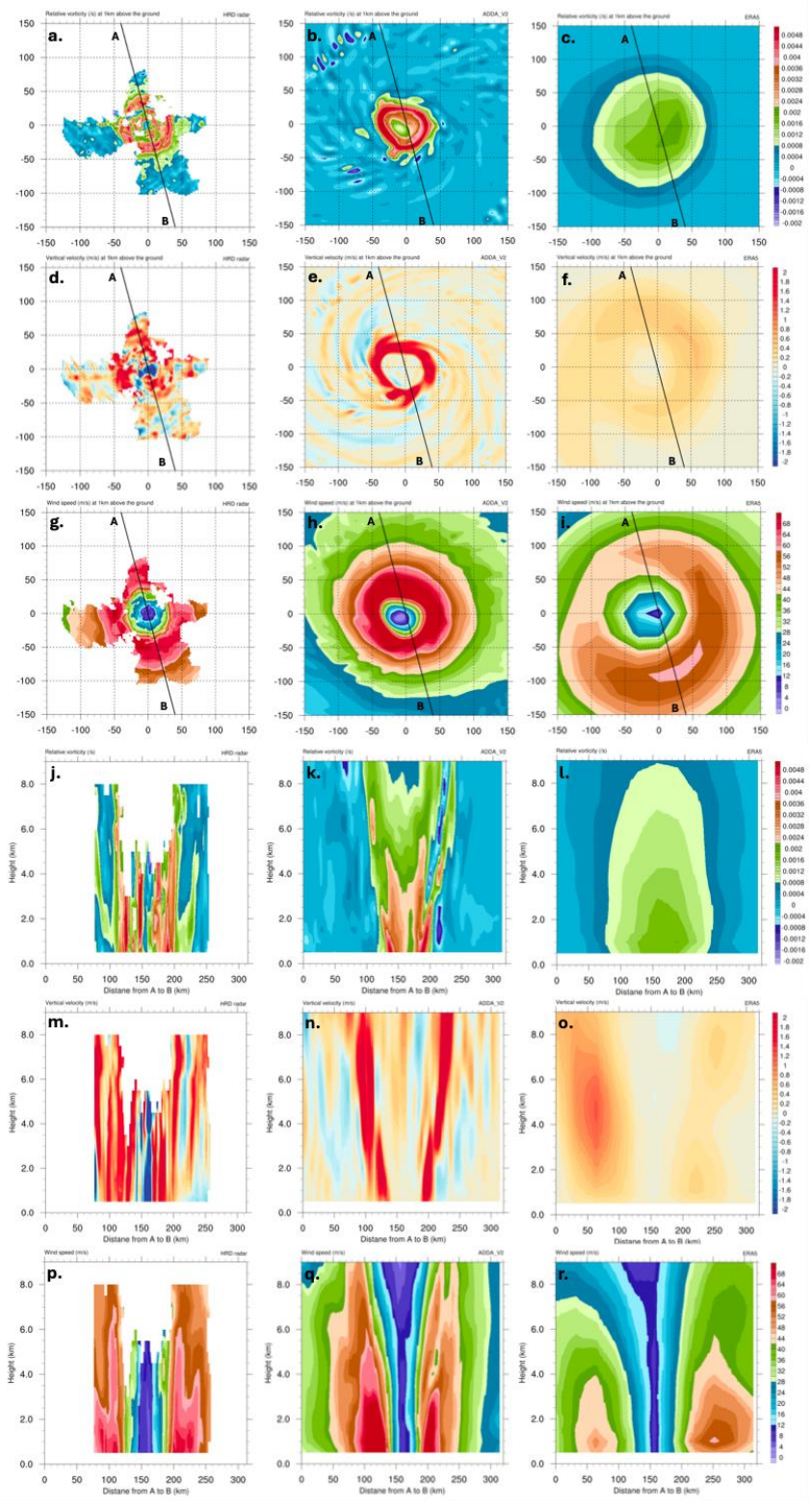

https://doi.org/10.5194/egusphere-2025-1805
Preprint. Discussion started: 11 June 2025

Figure 9. Horizontal distributions of (a)-(c) relative vorticity (s^{-1}), (d)-(f) vertical velocity (m s^{-1}), and (g)-(i) wind speed (m s^{-1}) in a 300 km × 300 km storm-centered coordinate. Vertical cross-sections along the lines displayed in (a)-(i) for (j)-(l) relative vorticity (s^{-1}), (m)-(o) vertical velocity (m s^{-1}), and (p)-(r) for (left column) TC-RADAR, (middle column) ADDA_v2, and (right column) ERA5 at 19 UTC on 14th September 2003 during Hurricane Isabel. The horizontal distribution is shown at 1-km above the ground.

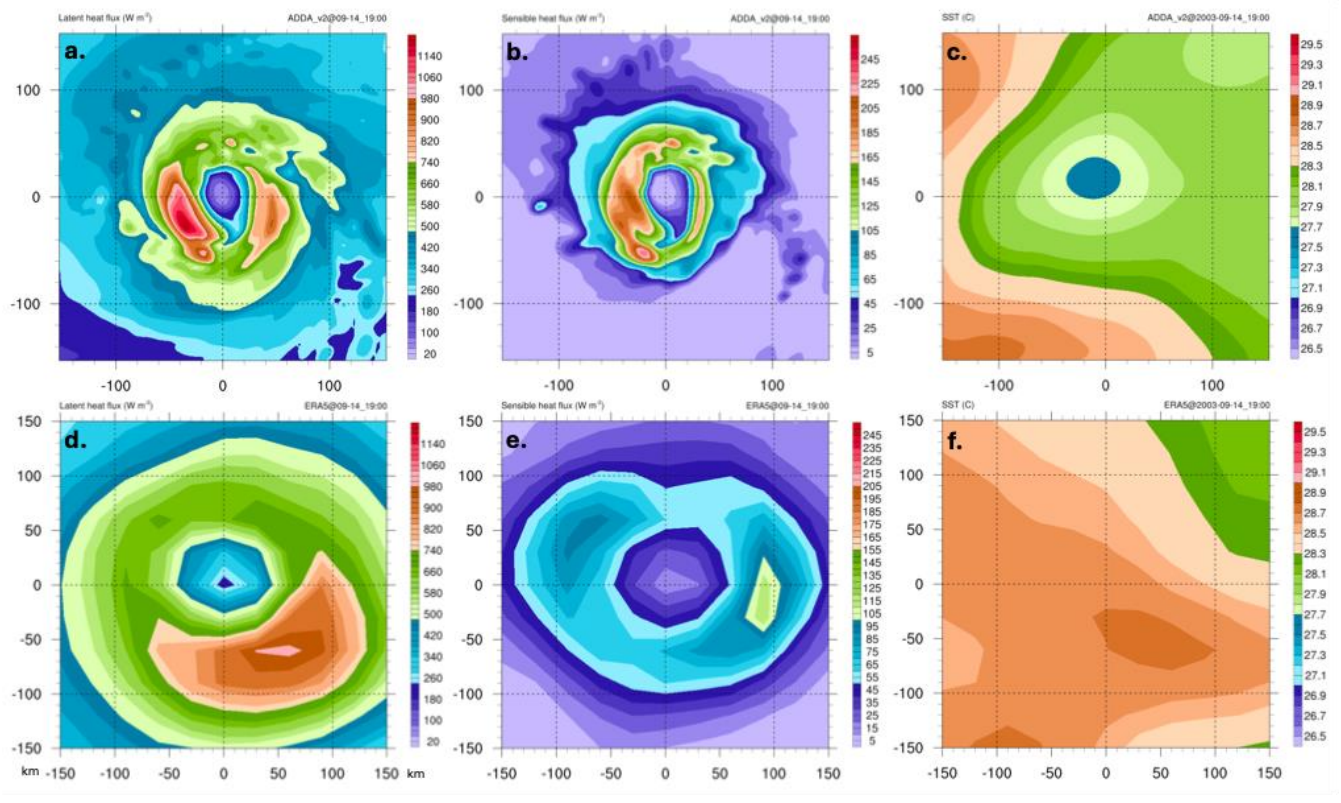

Figure 10. Horizontal distributions of (a),(d) latent heat flux (W m^{-2}), (b),(e) sensible heat flux (W m^{-2}), and (c),(f) sea surface temperature (℃) for (upper panel) ADDA_v2 and (lower panel) ERA5 at 19 UTC on 14th September 2003 during Hurricane Isabel. All the figures are displayed in a 300 km × 300 km storm-centered coordinate system.

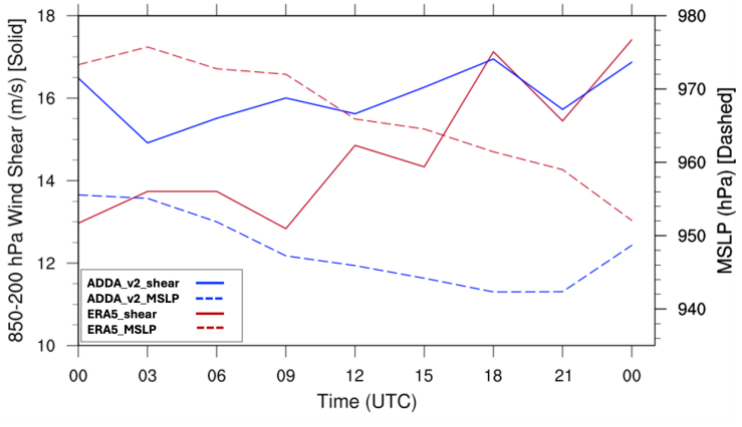

https://doi.org/10.5194/egusphere-2025-1805
Preprint. Discussion started: 11 June 2025

Figure 11. Time series of the magnitude of the 850-200 hPa vertical wind shear (m s^{-1}; solid lines) and minimum SLP (hPa; dashed lines) from 00 UTC on 14th September to 00 UTC on 15th September 2003, at 3-hour intervals. Red lines represent values from ERA5, while blue lines show values from ADDA_v2.

4 Summary and Discussions

This study demonstrates the skill of ADDA_v2 at representing TC climatology over much of the North Atlantic, Gulf of Mexico, and Caribbean Hurricane Basin over a 20-year period. We focus specifically on the advantages its high resolution provides over its coarser resolution forcing data (ERA5) in representing spatial, temporal and structural characteristics of TCs, demonstrating its potential for applications such as risk assessments for critical infrastructure.

Our results suggest that ADDA_V2 generates an overall more realistic depiction of TC characteristics and structure over a 20-year period. Over the full simulation, distributions of TC frequency and intensity are closer to observations than ERA5, as is the spatial distribution of TC centers. ADDA_v2 largely outperforms ERA5 at capturing the upper-tails of TC activity and intensity, indicating that allowing explicit convection can better capture mesoscale processes (here in the TC core) governing meteorological extremes (Akinsanola et al. 2024). For example, through composite analysis of the ten strongest TCs in ADDA_v2 and ERA5, we see ADDA_v2 is able to capture representatively intense TC (Category 4 versus Category 2 in ERA5), and exhibits realistic structural features that ERA5 often struggles to capture, such as a single, distinct warm core (Wang and Jiang, 2019) and a compact RMW (Bengsston et al., 2007; Schenkel and Hart, 2012; Li et al., 2017). By contrast, we find that ERA5 and ADDA_v2 show comparable skill at resolving the full distribution of minimum SLP, indicating that delineating TC intensity using a minimum SLP based scale (e.g. Klotzbach et al., 2020), instead of the traditional wind-based Saffir-Simpson scale may be more appropriate for ERA5 and other datasets at coarser spatial resolutions.

Nonetheless, ADDA_v2 does make improvements in capturing the most intense TC wind speeds, particularly those above Category 4, which - to our best knowledge - has yet to be observed in similar decadal CP-scale regional climate simulations to date. For example, Gutmann et al. (2018) did not simulate Category 4+ TCs in HRCONUS at a comparable resolution from 2001 to 2013. Although a full investigation into why ADDA_v2 captures such intensities is beyond the scope of this study—given substantial differences in boundary conditions, domain size, physical parameterizations, and tracking criteria—we can gain some preliminary insight by comparing the climatology of Category 4+ TCs over the subdomain and time period used in Gutmann et al., 2018. Within roughly the same domain, HURDAT2 recorded 13 total Category 4 TCs over Category 4 intensity while ADDA_v2 records 6, including qualitatively reasonable representations of Ivan (2004) and Earl (2010). Gutmann et al. (2018) attributed the absence of Category 4+ TCs in their simulations partly to the coarse resolution (~79 km; Dee et al., 2011) of ERA-Interim boundary conditions, which resulted in exclusively sub-hurricane strength TCs entering their study domain. This, combined with the very small over-ocean domain, may have reduced the opportunity for TCs to develop deep convection and intensify. By contrast, ADDA_v2 benefits from both finer forcing data (ERA5, ~31 km) and a larger over-ocean domain,

https://doi.org/10.5194/egusphere-2025-1805
Preprint. Discussion started: 11 June 2025

potentially allowing stronger TCs to be advected into the simulation and providing more time for intensification under convection-permitting conditions and warmer SSTs. However, other differences in model configuration may also contribute and warrant further investigation.

From the perspective of the underlying mechanisms behind ADDA_v2's improved performance, our case study of Hurricane Isabel (2003) provides important insight into the differences between CP and reanalysis datasets in capturing the same storm, particularly concerning its structures and physical processes, through a comparative analysis with observations. It is found that the different pathways between the two storms, despite similar environmental conditions, may be due to ADDA_v2's improved capability in capturing small-scale convection and finer details, which enhance vertical mixing, heat transfer, and energy exchange, leading to a more realistic representation of TCs. This supports our findings of improved TC representation on a climatological scale.

ADDA_v2's ability to accurately simulate these extreme TC winds, realistic RMWs and eyewall mesovortices exemplify its value for risk assessments of critical infrastructure in industries such as offshore wind and coastal building. ADDA_v2 could be used to calculate the return period of certain conditions such as an N-year return event, which may not be captured by ERA5. For example, Class I offshore wind turbines are not designed to withstand mean winds above 50 m s^{-1} or gusts above 70 m s^{-1} corresponding to TCs above Category 3 intensity (Worsnop et al., 2017), while Class T turbines can withstand average winds of up to 57 m s^{-1} (Wang et al., 2023). These speeds are consistently resolved by ADDA_v2, but are not present in ERA5. Additionally, ADDA_v2's composite TC suggests a far better representation of intense TC precipitation, which is a major key TC hazard for many communities.

For many regions in Mesoamerica and the Caribbean islands which lack a spatio-temporally continuous observational record and are not featured in other decadal scale CP simulations, assessing the climatology and risks from TCs is challenging. We note that ADDA_v2 performs particularly well in this region, capturing the same total number of TCs as HURDAT2 (157), while ERA5 identifies just 88. However, ADDA_v2 underrepresents major hurricanes by 10 compared to HURDAT2. Using ACE as a proxy for TC hazard exposure and dataset utility as it integrates frequency, intensity and duration over a spatial scale (Fig 12.), we find a comparable performance to the rest of basin even using a smaller bin size (1.5° bins vs 2.5° for the full domain), with ERA5 showing higher pattern correlation (0.91 vs. 0.75) but a larger RMSE (1.99 vs. 1.58). This suggests that while ERA5 better captures spatial distribution, ADDA_v2 more consistently resolves TC intensity. Notably, the RMSE difference between ADDA_v2 and ERA5 is reduced in this subregion compared to the full domain despite the smaller bin size, indicating that ADDA_v2 is particularly skillful at capturing strong TCs where observational data are sparse and the need for risk-informed planning is high.

https://doi.org/10.5194/egusphere-2025-1805
Preprint. Discussion started: 11 June 2025

While it is beyond the scope of this study to assess TC precipitation in Mesoamerica and the Caribbean Islands, ADDA_v2's ability to capture heavy TC precipitation in the eyewall suggests this as a possible use case. Indeed, Franco-Diaz et al., 2019 find that TCs contribute between 40 and 60% of extreme precipitation in coastal areas of Mexico using satellite estimates, however they note that these estimates tend to underpredict over land, especially in regions of complex terrain which characterize Mexico's coast. Furthermore, they find that coarse reanalysis datasets like ERA-Interim and JRA-55 underpredict the satellite precipitation. TC remnants in Mexico are often highly impactful despite their decaying intensity, with the orographic enhancement of remnants having the dual effect of causing costly and catastrophic flooding while providing much needed precipitation to arid inland regions that rely in part on TCs to replenish major reservoirs and recharge groundwater (Renteira-Villalobos and Hanson, 2025; Pedrozo-Acuña et al., 2014; Breña-Naranjo et al., 2015; Dominguez and Magaña, 2018). Future work may seek to address this further, with the intent of contributing data for risk analysis in these regions, which would benefit greatly from CP-scale assessment of inland TC precipitation.

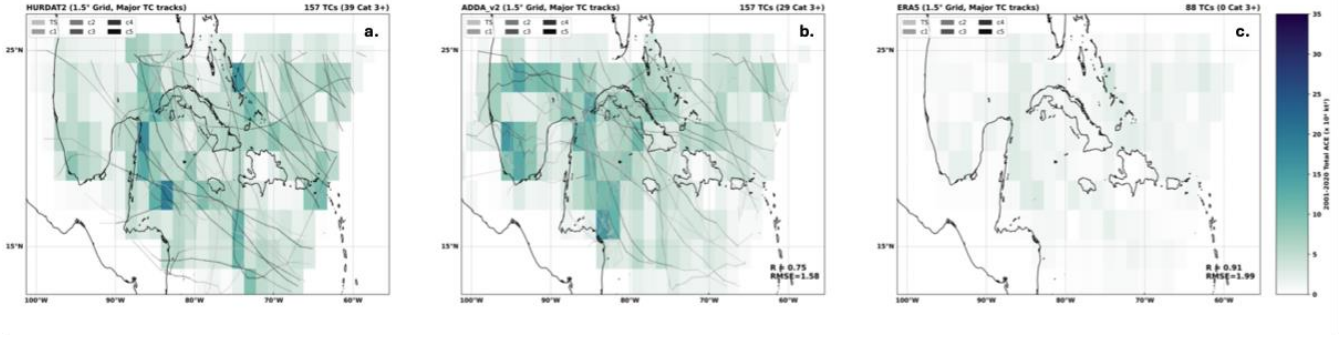

Figure 12: Total ACE and major (Category 3+) TC tracks over Mesoamerica and the Caribbean islands (101-55°W and 12.6-25°N) from 2001-2020 for (a) HURDAT2, (b) ADDA_v2 and (c) ERA5.

References

Agustín Breña-Naranjo, J., Pedrozo-Acuña, A., Pozos-Estrada, O., Jiménez-López, S. A., and López-López, M. R.: The contribution of tropical cyclones to rainfall in Mexico, Physics and Chemistry of the Earth, Parts A/B/C, 83–84, 111–122, https://doi.org/10.1016/j.pce.2015.05.011, 2015.

Akinsanola, A. A., Jung, C., Wang, J., and Kotamarthi, V. R.: Evaluation of precipitation across the contiguous United States, Alaska, and Puerto Rico in multi-decadal convection-permitting simulations, Sci Rep, 14, 1238, https://doi.org/10.1038/s41598-024-51714-3, 2024.

https://doi.org/10.5194/egusphere-2025-1805
Preprint. Discussion started: 11 June 2025

570 Atkinson, G. D. and Holliday, C. R.: Tropical Cyclone Minimum Sea Level Pressure/Maximum Sustained Wind
571 Relationship for the Western North Pacific, Monthly Weather Review, 105, 421–427, https://doi.org/10.1175/1520-
572 0493(1977)105<0421:TCMINIMUM SLP>2.0.CO;2, 1977.

573 Balaguru, K., Xu, W., Chang, C.-C., Leung, L. R., Judi, D. R., Hagos, S. M., Wehner, M. F., Kossin, J. P., and Ting, M.:
574 Increased U.S. coastal hurricane risk under climate change, Science Advances, 9, eadf0259,
575 https://doi.org/10.1126/sciadv.adf0259, 2023.

576 Bengtsson, L., Hodges ,K. I., and and Esch, M.: Tropical cyclones in a T159 resolution global climate model: comparison
577 with observations and re-analyses, Tellus A: Dynamic Meteorology and Oceanography, 59, 396–416,
578 https://doi.org/10.1111/j.1600-0870.2007.00236.x, 2007.

579 Bi, M., Wang, R., Li, T., and Ge, X.: Effects of vertical shear on intensification of tropical cyclones of different initial sizes,
580 Front. Earth Sci., 11, https://doi.org/10.3389/feart.2023.1106204, 2023.

581 Bian, G., Tang, J., Wang, S., and Fang, J.: Regional climate simulation of tropical cyclone at gray-zone resolution over
582 western North Pacific: with/without cumulus parameterization, Clim Dyn, 61, 3179–3194, https://doi.org/10.1007/s00382-
583 023-06740-8, 2023.

584 Bié, A. J. and de Camargo, R.: Tropical cyclones position and intensity in the Southwest Indian Ocean as represented by
585 CFS and ERA5 atmospheric reanalysis datasets, International Journal of Climatology, 43, 4532–4551,
586 https://doi.org/10.1002/joc.8101, 2023.

587 Bourdin, S., Fromang, S., Dulac, W., Cattiaux, J., and Chauvin, F.: Intercomparison of four algorithms for detecting tropical
588 cyclones using ERA5, Geoscientific Model Development, 15, 6759–6786, https://doi.org/10.5194/gmd-15-6759-2022,
589 2022.

590 Braun, S. A. and Wu, L.: A Numerical Study of Hurricane Erin (2001). Part II: Shear and the Organization of Eyewall
591 Vertical Motion, https://doi.org/10.1175/MWR3336.1, 2007.

592 Catto, J. L., Shaffrey, L. C., and Hodges, K. I.: Can Climate Models Capture the Structure of Extratropical Cyclones?,
593 https://doi.org/10.1175/2009JCLI3318.1, 2010.

594 Chand, S. S., Walsh, K. J. E., Camargo, S. J., Kossin, J. P., Tory, K. J., Wehner, M. F., Chan, J. C. L., Klotzbach, P. J.,
595 Dowdy, A. J., Bell, S. S., Ramsay, H. A., and Murakami, H.: Declining tropical cyclone frequency under global warming,
596 Nat. Clim. Chang., 12, 655–661, https://doi.org/10.1038/s41558-022-01388-4, 2022.

597 Chen, S. S., Price, J. F., Zhao, W., Donelan, M. A., and Walsh, E. J.: The CBLAST-Hurricane Program and the Next-
598 Generation Fully Coupled Atmosphere–Wave–Ocean Models for Hurricane Research and Prediction, Bulletin of the
599 American Meteorological Society, 88, 311–317, 2007.

https://doi.org/10.5194/egusphere-2025-1805
Preprint. Discussion started: 11 June 2025

Dominguez, C. and Magaña, V.: The role of tropical cyclones in precipitation over the tropical and subtropical North America, Frontiers in Earth Science, 6, 19, 2018.

Dullaart, J. C. M., Muis, S., Bloemendaal, N., and Aerts, J. C. J. H.: Advancing global storm surge modelling using the new ERA5 climate reanalysis, Clim Dyn, 54, 1007–1021, https://doi.org/10.1007/s00382-019-05044-0, 2020.

Eley, E. N., Subrahmanyam, B., and Trott, C. B.: Ocean–Atmosphere Interactions during Hurricanes Marco and Laura (2020), Remote Sensing, 13, 1932, https://doi.org/10.3390/rs13101932, 2021.

Faranda, D., Messori, G., Bourdin, S., Vrac, M., Thao, S., Riboldi, J., Fromang, S., and Yiou, P.: Correcting biases in tropical cyclone intensities in low-resolution datasets using dynamical systems metrics, Clim Dyn, 61, 4393–4409, https://doi.org/10.1007/s00382-023-06794-8, 2023.

Fischer, M. S., Reasor, P. D., Rogers, R. F., and Gamache, J. F.: An Analysis of Tropical Cyclone Vortex and Convective Characteristics in Relation to Storm Intensity Using a Novel Airborne Doppler Radar Database, https://doi.org/10.1175/MWR-D-21-0223.1, 2022.

Franco-Díaz, A., Klingaman, N. P., Vidale, P. L., Guo, L., and Demory, M.-E.: The contribution of tropical cyclones to the atmospheric branch of Middle America's hydrological cycle using observed and reanalysis tracks, Clim Dyn, 53, 6145–6158, https://doi.org/10.1007/s00382-019-04920-z, 2019.

Gensini, V. A., Haberlie, A. M., and Ashley, W. S.: Convection-permitting simulations of historical and possible future climate over the contiguous United States, Clim Dyn, 60, 109–126, https://doi.org/10.1007/s00382-022-06306-0, 2023.

Gentry, M. S. and Lackmann, G. M.: Sensitivity of Simulated Tropical Cyclone Structure and Intensity to Horizontal Resolution, https://doi.org/10.1175/2009MWR2976.1, 2010.

Gori, A., Lin, N., and Xi, D.: Tropical Cyclone Compound Flood Hazard Assessment: From Investigating Drivers to Quantifying Extreme Water Levels, Earth's Future, 8, e2020EF001660, https://doi.org/10.1029/2020EF001660, 2020.

Hallowell, S. T., Myers, A. T., Arwade, S. R., Pang, W., Rawal, P., Hines, E. M., Hajjar, J. F., Qiao, C., Valamanesh, V., Wei, K., Carswell, W., and Fontana, C. M.: Hurricane risk assessment of offshore wind turbines, Renewable Energy, 125, 234–249, https://doi.org/10.1016/j.renene.2018.02.090, 2018.

Hazelton, A. T., Harris, L., and Lin, S.-J.: Evaluation of Tropical Cyclone Structure Forecasts in a High-Resolution Version of the Multiscale GFDL fvGFS Model, https://doi.org/10.1175/WAF-D-17-0140.1, 2018.

Hernández Ayala, J. J. and and Matyas, C. J.: Spatial distribution of tropical cyclone rainfall and its contribution to the climatology of Puerto Rico, Physical Geography, 39, 1–20, https://doi.org/10.1080/02723646.2017.1354416, 2018.

https://doi.org/10.5194/egusphere-2025-1805
Preprint. Discussion started: 11 June 2025

Hernández Ayala, J. J., Keellings ,David, Waylen ,Peter R., and and Matyas, C. J.: Extreme floods and their relationship with tropical cyclones in Puerto Rico, Hydrological Sciences Journal, 62, 2103–2119, https://doi.org/10.1080/02626667.2017.1368521, 2017.

Hersbach, H., Bell, B., Berrisford, P., Hirahara, S., Horányi, A., Muñoz-Sabater, J., Nicolas, J., Peubey, C., Radu, R., Schepers, D., Simmons, A., Soci, C., Abdalla, S., Abellan, X., Balsamo, G., Bechtold, P., Biavati, G., Bidlot, J., Bonavita, M., De Chiara, G., Dahlgren, P., Dee, D., Diamantakis, M., Dragani, R., Flemming, J., Forbes, R., Fuentes, M., Geer, A., Haimberger, L., Healy, S., Hogan, R. J., Hólm, E., Janisková, M., Keeley, S., Laloyaux, P., Lopez, P., Lupu, C., Radnoti, G., de Rosnay, P., Rozum, I., Vamborg, F., Villaume, S., and Thépaut, J.-N.: The ERA5 global reanalysis, Quarterly Journal of the Royal Meteorological Society, 146, 1999–2049, https://doi.org/10.1002/qj.3803, 2020.

Hidalgo, H. G., Alfaro, E. J., HernÃandez-Castro, F., and Pérez-Briceño, P. M.: Identification of Tropical Cyclones' Critical Positions Associated with Extreme Precipitation Events in Central America, Atmosphere, 11, 1123, https://doi.org/10.3390/atmos11101123, 2020.

Hodges, K., Cobb, A., and Vidale, P. L.: How Well Are Tropical Cyclones Represented in Reanalysis Datasets?, https://doi.org/10.1175/JCLI-D-16-0557.1, 2017.

Hsu, S. A. and Yan, Z.: A Note on the Radius of Maximum Wind for Hurricanes, Journal of Coastal Research, 14, 1998.

Hsu, W.-C., Kooperman, G. J., Hannah, W. M., Reed, K. A., Akinsanola, A. A., and Pendergrass, A. G.: Evaluating Mesoscale Convective Systems Over the US in Conventional and Multiscale Modeling Framework Configurations of E3SMv1, Journal of Geophysical Research: Atmospheres, 128, e2023JD038740, https://doi.org/10.1029/2023JD038740, 2023.

Islam, M. R., Lee, C.-Y., Mandli, K. T., and Takagi, H.: A new tropical cyclone surge index incorporating the effects of coastal geometry, bathymetry and storm information, Sci Rep, 11, 16747, https://doi.org/10.1038/s41598-021-95825-7, 2021.

Institute, F. M. IHO Sea Areas, version 3. Available online at https://www.marineregions.org/. https://doi.org/10.14284/323, 2018.

Jacob, D., Petersen, J., Eggert, B., Alias, A., Christensen, O. B., Bouwer, L. M., Braun, A., Colette, A., Déqué, M., Georgievski, G., Georgopoulou, E., Gobiet, A., Menut, L., Nikulin, G., Haensler, A., Hempelmann, N., Jones, C., Keuler, K., Kovats, S., Kröner, N., Kotlarski, S., Kriegsmann, A., Martin, E., Van Meijgaard, E., Moseley, C., Pfeifer, S., Preuschmann, S., Radermacher, C., Radtke, K., Rechid, D., Rounsevell, M., Samuelsson, P., Somot, S., Soussana, J.-F., Teichmann, C., Valentini, R., Vautard, R., Weber, B., and Yiou, P.: EURO-CORDEX: new high-resolution climate change projections for European impact research, Reg Environ Change, 14, 563–578, https://doi.org/10.1007/s10113-013-0499-2, 2014.

https://doi.org/10.5194/egusphere-2025-1805
Preprint. Discussion started: 11 June 2025

Jones, E., Wing, A. A., and Parfitt, R.: A global perspective of tropical cyclone precipitation in reanalyses, Journal of Climate, 34, 8461–8480, 2021.

Jung, C. and Lackmann, G. M.: The Response of Extratropical Transition of Tropical Cyclones to Climate Change: Quasi-Idealized Numerical Experiments, https://doi.org/10.1175/JCLI-D-20-0543.1, 2021.

Jung, C. and Lackmann, G. M.: Changes in Tropical Cyclones Undergoing Extratropical Transition in a Warming Climate: Quasi-Idealized Numerical Experiments of North Atlantic Landfalling Events, Geophysical Research Letters, 50, e2022GL101963, https://doi.org/10.1029/2022GL101963, 2023.

Kanada, S. and Wada, A.: Sensitivity to Horizontal Resolution of the Simulated Intensifying Rate and Inner-Core Structure of Typhoon Ida, an Extremely Intense Typhoon, Journal of the Meteorological Society of Japan. Ser. II, 94A, 181–190, https://doi.org/10.2151/jmsj.2015-037, 2016.

Kanada, S., Tsuboki, K., and Takayabu, I.: Future Changes of Tropical Cyclones in the Midlatitudes in 4-km-mesh Downscaling Experiments from Large-Ensemble Simulations, Sola, 16, 57–63, https://doi.org/10.2151/sola.2020-010, 2020.

Klotzbach, P. J., Bell, M. M., Bowen, S. G., Gibney, E. J., Knapp, K. R., and Schreck, C. J.: Surface Pressure a More Skillful Predictor of Normalized Hurricane Damage than Maximum Sustained Wind, https://doi.org/10.1175/BAMS-D-19-0062.1, 2020.

Klotzbach, P. J., Chavas, D. R., Bell, M. M., Bowen, S. G., Gibney, E. J., and Schreck III, C. J.: Characterizing Continental US Hurricane Risk: Which Intensity Metric Is Best?, Journal of Geophysical Research: Atmospheres, 127, e2022JD037030, https://doi.org/10.1029/2022JD037030, 2022.

Knapp, K. R. and Kruk, M. C.: Quantifying Interagency Differences in Tropical Cyclone Best-Track Wind Speed Estimates, https://doi.org/10.1175/2009MWR3123.1, 2010.

Knapp, K. R., Kruk, M. C., Levinson, D. H., Diamond, H. J., and Neumann, C. J.: The International Best Track Archive for Climate Stewardship (IBTrACS), https://doi.org/10.1175/2009BAMS2755.1, 2010.

Knutson, T., Camargo, S. J., Chan, J. C. L., Emanuel, K., Ho, C.-H., Kossin, J., Mohapatra, M., Satoh, M., Sugi, M., Walsh, K., and Wu, L.: Tropical Cyclones and Climate Change Assessment: Part II: Projected Response to Anthropogenic Warming, https://doi.org/10.1175/BAMS-D-18-0194.1, 2020.

Knutson, T. R., McBride, J. L., Chan, J., Emanuel, K., Holland, G., Landsea, C., Held, I., Kossin, J. P., Srivastava, A. K., and Sugi, M.: Tropical cyclones and climate change, Nature Geoscience, 3, 157–163, https://doi.org/10.1038/ngeo779, 2010.

Knutson, T. R., Chung, M. V., Vecchi, G., Sun, J., Hsieh, T.-L., and Smith, A. J. P.: Climate change is probably increasing the intensity of tropical cyclones, n.d.

https://doi.org/10.5194/egusphere-2025-1805
Preprint. Discussion started: 11 June 2025

Kossin, J. P. and Schubert, W. H.: Mesovortices, Polygonal Flow Patterns, and Rapid Pressure Falls in Hurricane-Like Vortices, 2001.

Kossin, J. P. and Schubert, W. H.: Mesovortices in Hurricane Isabel, Bulletin of the American Meteorological Society, 85, 151–153, 2004.

Landsea, C. W. and Franklin, J. L.: Atlantic Hurricane Database Uncertainty and Presentation of a New Database Format, https://doi.org/10.1175/MWR-D-12-00254.1, 2013.

Li, J., Pan, S., Chen, Y., and Pan, Y.: Assessment of Tropical Cyclones in Ecmwf Reanalysis Data over Northwest Pacific Ocean, n.d.

Liu, C., Ikeda, K., Rasmussen, R., Barlage, M., Newman, A. J., Prein, A. F., Chen, F., Chen, L., Clark, M., Dai, A., Dudhia, J., Eidhammer, T., Gochis, D., Gutmann, E., Kurkute, S., Li, Y., Thompson, G., and Yates, D.: Continental-scale convection-permitting modeling of the current and future climate of North America, Clim Dyn, 49, 71–95, https://doi.org/10.1007/s00382-016-3327-9, 2017.

Manganello, J. V., Hodges, K. I., Kinter, J. L., Cash, B. A., Marx, L., Jung, T., Achuthavarier, D., Adams, J. M., Altshuler, E. L., Huang, B., Jin, E. K., Stan, C., Towers, P., and Wedi, N.: Tropical Cyclone Climatology in a 10-km Global Atmospheric GCM: Toward Weather-Resolving Climate Modeling, https://doi.org/10.1175/JCLI-D-11-00346.1, 2012.

Moon, I.-J., Kim, S.-H., and Chan, J. C. L.: Climate change and tropical cyclone trend, Nature, 570, E3–E5, https://doi.org/10.1038/s41586-019-1222-3, 2019.

Murakami, H.: Tropical cyclones in reanalysis data sets, Geophysical Research Letters, 41, 2133–2141, https://doi.org/10.1002/2014GL059519, 2014.

Murakami, H., Delworth, T. L., Cooke, W. F., Zhao, M., Xiang, B., and Hsu, P.-C.: Detected climatic change in global distribution of tropical cyclones, Proceedings of the National Academy of Sciences, 117, 10706–10714, https://doi.org/10.1073/pnas.1922500117, 2020.

Pedrozo - Acuña, A., Breña - Naranjo, J. A., and Domínguez - Mora, R.: The hydrological setting of the 2013 floods in Mexico, Weather (00431656), 69, 295–302, https://doi.org/10.1002/wea.2355, 2014.

Powell, M. D. and Reinhold, T. A.: Tropical Cyclone Destructive Potential by Integrated Kinetic Energy, https://doi.org/10.1175/BAMS-88-4-513, 2007.

Prein, A. F., Langhans, W., Fosser, G., Ferrone, A., Ban, N., Goergen, K., Keller, M., Tölle, M., Gutjahr, O., Feser, F., Brisson, E., Kollet, S., Schmidli, J., van Lipzig, N. P. M., and Leung, R.: A review on regional convection-permitting climate modeling: Demonstrations, prospects, and challenges, Reviews of Geophysics, 53, 323–361, https://doi.org/10.1002/2014RG000475, 2015.

https://doi.org/10.5194/egusphere-2025-1805
Preprint. Discussion started: 11 June 2025

Rasmussen, R. M., Chen, F., Liu, C. H., Ikeda, K., Prein, A., Kim, J., Schneider, T., Dai, A., Gochis, D., Dugger, A., Zhang, Y., Jaye, A., Dudhia, J., He, C., Harrold, M., Xue, L., Chen, S., Newman, A., Dougherty, E., Abolafia-Rosenzweig, R., Lybarger, N. D., Viger, R., Lesmes, D., Skalak, K., Brakebill, J., Cline, D., Dunne, K., Rasmussen, K., and Miguez-Macho, G.: CONUS404: The NCAR–USGS 4-km Long-Term Regional Hydroclimate Reanalysis over the CONUS, https://doi.org/10.1175/BAMS-D-21-0326.1, 2023.

Reed, K. A., Wehner, M. F., and Zarzycki, C. M.: Attribution of 2020 hurricane season extreme rainfall to human-induced climate change, Nat Commun, 13, 1905, https://doi.org/10.1038/s41467-022-29379-1, 2022.

Renteria-Villalobos, M. and Hanson, R. T.: Capturing wetness for sustainability from climate variability and change in the Rio Conchos, Chihuahua, Mexico, Journal of Hydrology: Regional Studies, 58, 102256, https://doi.org/10.1016/j.ejrh.2025.102256, 2025.

Roberts, M. J., Camp, J., Seddon, J., Vidale, P. L., Hodges, K., Vannière, B., Mecking, J., Haarsma, R., Bellucci, A., Scoccimarro, E., Caron, L.-P., Chauvin, F., Terray, L., Valcke, S., Moine, M.-P., Putrasahan, D., Roberts, C. D., Senan, R., Zarzycki, C., Ullrich, P., Yamada, Y., Mizuta, R., Kodama, C., Fu, D., Zhang, Q., Danabasoglu, G., Rosenbloom, N., Wang, H., and Wu, L.: Projected Future Changes in Tropical Cyclones Using the CMIP6 HighResMIP Multimodel Ensemble, Geophysical Research Letters, 47, e2020GL088662, https://doi.org/10.1029/2020GL088662, 2020.

Schenkel, B. A. and Hart, R. E.: An Examination of Tropical Cyclone Position, Intensity, and Intensity Life Cycle within Atmospheric Reanalysis Datasets, https://doi.org/10.1175/2011JCLI4208.1, 2012.

Schreck, C. J., Knapp, K. R., and Kossin, J. P.: The Impact of Best Track Discrepancies on Global Tropical Cyclone Climatologies using IBTrACS, https://doi.org/10.1175/MWR-D-14-00021.1, 2014.

Schultz, L. A. and Cecil, D. J.: Tropical Cyclone Tornadoes, 1950–2007, https://doi.org/10.1175/2009MWR2896.1, 2009.

Sharmila, S. and Walsh, K. J. E.: Recent poleward shift of tropical cyclone formation linked to Hadley cell expansion, Nature Clim Change, 8, 730–736, https://doi.org/10.1038/s41558-018-0227-5, 2018.

Slocum, C. J., Razin, M. N., Knaff, J. A., and Stow, J. P.: Does ERA5 Mark a New Era for Resolving the Tropical Cyclone Environment?, https://doi.org/10.1175/JCLI-D-22-0127.1, 2022.

Smith, A. B.: NOAA National Centers for Environmental Information (NCEI) US Billion-Dollar Weather and Climate Disasters, NOAA National Centers for Environmental Information (NCEI), https://www. ncei. noaa. gov/access/billions/(last accessed: 30 June 2024), 2023.

Stansfield, A. M. and Reed, K. A.: Global tropical cyclone precipitation scaling with sea surface temperature, npj Clim Atmos Sci, 6, 1–10, https://doi.org/10.1038/s41612-023-00391-6, 2023.

https://doi.org/10.5194/egusphere-2025-1805
Preprint. Discussion started: 11 June 2025

Steptoe, H., Savage, N. H., Sadri, S., Salmon, K., Maalick, Z., and Webster, S.: Tropical cyclone simulations over Bangladesh at convection permitting 4.4 km & 1.5 km resolution, Sci Data, 8, 62, https://doi.org/10.1038/s41597-021-00847-5, 2021.

Stern, D. P. and Nolan, D. S.: Reexamining the Vertical Structure of Tangential Winds in Tropical Cyclones: Observations and Theory, https://doi.org/10.1175/2009JAS2916.1, 2009.

Tang, B. H., Rios-Berrios, R., and Zhang, J. A.: Diagnosing Radial Ventilation in Dropsonde Observations of Hurricane Sam (2021), https://doi.org/10.1175/MWR-D-23-0224.1, 2024.

Torn, R. D. and Snyder, C.: Uncertainty of Tropical Cyclone Best-Track Information, https://doi.org/10.1175/WAF-D-11-00085.1, 2012.

Tu, S., Chan, J. C. L., Xu, J., Zhong, Q., Zhou, W., and Zhang, Y.: Increase in tropical cyclone rain rate with translation speed, Nat Commun, 13, 7325, https://doi.org/10.1038/s41467-022-35113-8, 2022.

Ullrich, P. A. and Zarzycki, C. M.: TempestExtremes: A framework for scale-insensitive pointwise feature tracking on unstructured grids, Geoscientific Model Development, 10, 1069–1090, 2017.

Ullrich, P. A., Zarzycki, C. M., McClenny, E. E., Pinheiro, M. C., Stansfield, A. M., and Reed, K. A.: TempestExtremes v2.1: A community framework for feature detection, tracking, and analysis in large datasets, Geoscientific Model Development, 14, 5023–5048, 2021.

Vecchi, G. A., Landsea, C., Zhang, W., Villarini, G., and Knutson, T.: Changes in Atlantic major hurricane frequency since the late-19th century, Nat Commun, 12, 4054, https://doi.org/10.1038/s41467-021-24268-5, 2021.

Villarini, G. and Vecchi, G. A.: North Atlantic Power Dissipation Index (PDI) and Accumulated Cyclone Energy (ACE): Statistical Modeling and Sensitivity to Sea Surface Temperature Changes, https://doi.org/10.1175/JCLI-D-11-00146.1, 2012.

Wang, J., Deskos, G., Pringle, W. J., Haupt, S. E., Feng, S., Berg, L. K., Churchfield, M., Biswas, M., Musial, W., Muradyan, P., Hendricks, E., Kotamarthi, R., Xue, P., Rozoff, C. M., and Bryan, G.: Impact of Tropical and Extratropical Cyclones on Future U.S. Offshore Wind Energy, https://doi.org/10.1175/BAMS-D-24-0080.1, 2024.

Wang, X. and Jiang, H.: A 13-Year Global Climatology of Tropical Cyclone Warm-Core Structures from AIRS Data, https://doi.org/10.1175/MWR-D-18-0276.1, 2019.

Wang, Y.: Vortex Rossby Waves in a Numerically Simulated Tropical Cyclone. Part II: The Role in Tropical Cyclone Structure and Intensity Changes, 2002.

https://doi.org/10.5194/egusphere-2025-1805
Preprint. Discussion started: 11 June 2025

Wehner, M. F., Zarzycki, C., and Patricola, C.: Estimating the Human Influence on Tropical Cyclone Intensity as the Climate Changes, in: Hurricane Risk, edited by: Collins, J. M. and Walsh, K., Springer International Publishing, Cham, 235–260, https://doi.org/10.1007/978-3-030-02402-4_12, 2019.

Worsnop, R. P., Lundquist, J. K., Bryan, G. H., Damiani, R., and Musial, W.: Gusts and shear within hurricane eyewalls can exceed offshore wind turbine design standards, Geophysical Research Letters, 44, 6413–6420, https://doi.org/10.1002/2017GL073537, 2017.

Yan, L., Guo, H., Peterka, T., Wang, B., and Wang, J.: TROPHY: A Topologically Robust Physics-Informed Tracking Framework for Tropical Cyclones, IEEE Transactions on Visualization and Computer Graphics, 30, 1249–1259, https://doi.org/10.1109/TVCG.2023.3326905, 2024.

Zarzycki, C. M. and Ullrich, P. A.: Assessing sensitivities in algorithmic detection of tropical cyclones in climate data, Geophysical Research Letters, 44, 1141–1149, https://doi.org/10.1002/2016GL071606, 2017.

Zhang, G., Murakami, H., Knutson, T. R., Mizuta, R., and Yoshida, K.: Tropical cyclone motion in a changing climate, Science Advances, 6, eaaz7610, https://doi.org/10.1126/sciadv.aaz7610, 2020.